Translatomic database of cortical astroglia across male and female mouse development reveals two distinct developmental phenotypes

Gareth M. Rurak[1], Stephanie Simard[1], François Charih[4], Amanda Van Geel[1], John Stead[1], Barbara Woodside[1,3], James R. Green[4], Gianfilippo Coppola*[2], Natalina Salmaso*[1,2]

Running Title:

Affiliations: 1-Department of Neuroscience, Carleton University, Ottawa, Ontario;
2-Department of Pathology, Yale University; 3- Concordia University, Montreal, Quebec
4-Department of Systems and Computer Engineering, Carleton University, Ottawa, Ontario

*co-senior authors

Author for Correspondence:

Natalina Salmaso

Carleton University, 1125 Colonel By Drive, Ottawa, Ontario, K1S 5B6, Canada

Tel: 613-520 2600

Email: natalina.salmaso@carleton.ca

Gianfilippo Coppola

Yale University, 310 Cedar Street, New Haven, CT 06520-8023, USA

Email: gianfilippo.coppola@yale.edu

Abstract

Astroglial cells are emerging as key players in the development and homeostatic maintenance of neurons and neuronal networks. Astroglial cell functions are critical to neuronal migration and maturation, myelination, and synapse dynamics, however little is known about astroglial phenotypic changes over development. Furthermore, astroglial cells express steroid hormone receptors and show rapid responses to hormonal manipulations, however, despite important sex differences in telencephalic regions such as the cortex and hippocampus few studies have examined sex differences in astroglial cells in development and outside of the hypothalamus and amygdala. To phenotype cortical astroglial cells across postnatal development while considering potential sex differences, we used translating ribosome affinity purification together with RNA sequencing (TRAPseq) and immunohistochemistry to phenotype the entire astroglial translatome in males and females at key developmental time points: P1, P4, P7, P14, P35 and in adulthood. We found that although astroglia show few sex differences in adulthood, they show significant sex differences in developmental gene expression patterns between at P1, P7 and P35, that suggests sex differences in developmental functions. We also found two distinct astroglial phenotypes between early (P1-P7) and late development (P14-Adult). Together these data clearly delineate and phenotype astroglia across development and identify sex differences in astroglial developmental programs that could have an important impact on the construction and maintenance of neuronal networks and related behavioural phenotypes.

Acknowledgements

We would like to thank our funding providers, the Carleton University Discovery Grant to N.S., Natural Sciences and Engineering Research Council of Canada Discovery Grant to N.S., the Canadian Foundation for Innovation to N.S., and the Canadian Research Chairs to N.S..

We thank Dr. Julianna Tomlinson, Dr. Michael Schlossmacher and his laboratory members at the University of Ottawa for providing us with infrastructural support and more. Finally, we would like to thank Dr. Alfonso Abizaid for his invaluable input into the planning and preparation of this research project.

Introduction

The cerebral cortex is a complex network of layered neuronal cells that uses a balance of excitatory and inhibitory signals to communicate both within the cerebral cortex itself and to lower brain regions[1]. It is the most recently evolved component of the mammalian central nervous system and is uniquely involved in higher order cognitive functions[2] that are central to intelligence and emotional processing. The complex layered structure of the cerebral cortex emerges during embryonic development in an "inside-out" pattern consisting of radial glial cell (RGC)-assisted neuroblast migration to lower layers (i.e. VI) before the upper layers are formed [3,4]. The appropriate migration of developing neuroblasts is an integral part of the maturation of the cerebral cortex. Early insults or perturbations during this critical period of development may disrupt the gross organization of excitatory and inhibitory networks leading to neurodevelopmental disorders including autism spectrum disorders (ASD) or schizophrenia, and mood disorders such as bipolar disorder[5,6]. Importantly, even subtle modifications in the number or functionality of cortical synapses may lead to serious behavioural consequences and have been related to a number of psychiatric diseases[7].

The prevalence of many, if not all, neurodevelopmental disorders and mood disorders related to cortical function are sexually dimorphic in human populations[8] .Thus understanding sex differences in the organization and function of the cerebral cortex is critical to understanding the neurodevelopmental underpinnings of psychiatric disease. There is a great deal of literature that suggests that gonadal hormones can directly modulate disease states associated with schizophrenia, anxiety and mood disorders[9,10]. Similarly, in rodent models, basal changes in behaviours such as in the forced swim task have been demonstrated across the estrous cycle[11]. Together, these data support an important role for ovarian hormones and in particular, estrogen, in mediating those behaviours related to higher order cognitive functioning in situ. Effects on behaviour and physiology that depend on current levels of hormones such as those described above are referred to as activational. The sex steroid milieu of embryonic and neonatal life, however, can also have organizational effects. These are changes induced in this early stage of development that persist even when the hormonal state producing them has dissipated.

Testosterone secreted from the testes of XY-male embryos acting either directly or via aromatisation to estradiol is the primary organizing influence in the sexual differentiation of the brain[12,13]; The role of estradiol in mediating organizational sex differences through neuronal estrogen receptor (ERs) signaling has been extensively studied in the hypothalamus and amygdala. For example, in the medial pre-optic area (MPOA), estrogen receptor signalling induces prostaglandin-mediated synapse formation through microglial and astroglial-mediated functions[13]. Neuroanatomical and functional sex differences are also well defined in various neuronal populations of the hypothalamus[14], amygdala[15], and hippocampus[16]. The cerebral cortex, however, has received less attention than other telencephalic regions[17].

While it is possible that sex differences in cortical network functioning may be completely mediated by direct hormonal modulation, sex differences in prevalence of anxiety disorders[9] and ASD[18] are apparent prior to puberty, and pro-dromal behaviours associated with psychosis also show sex differences early in development[19], suggesting that organizational sex differences (presumably in cortical networks) may be involved in differences in risk or vulnerability for psychiatric disease.

Astroglial cells have recently emerged as key mediators in brain development and the etiology of neurodevelopmental and mood disorders has been related to astroglial-mediated functions such as neuroblast migration and synapse formation, maturation, and elimination[20,21]. Cortical astroglial cells are a heterogenous cell population traditionally categorised into three main subtypes easily distinguished by morphology, although recent work has suggested that many more subtypes exist when astroglial cells are categorised through single cell RNASeq or other gene and protein expression methods[22,23]. The first subtype of astroglial cells to emerge in development are RGCs[24]. In addition to providing scaffolding for migrating neuroblasts, astroglial cells exhibit stem-like potential in early development and following injury that allows them to give rise to other neuronal cells before maturing and populating the cortex as fibrous or protoplasmic astroglial cells[25,26]. As astroglia mature, their stem cell potential diminishes, as marked by an increase in glutamate synthetase and decreased expression of Sox2 and vimentin[27]. The two main mature morphological subtypes in the cortex are characterized as protoplasmic; canonical

astroglia with large domains of many fine processes, and fibrous; astroglial cells with many long fibrous extensions[28]. These mature astroglial cell populations are responsible for the construction and maintenance of both excitatory[29] and inhibitory[30] synapses in the developing neocortex, modulating neuron signaling and maturation[31], and the elimination of synapses during cortical maturation[21]. Work from the Barres laboratory characterised astroglial cells in brain development using next generation sequencing techniques, however these studies did not examine the contributions of biological sex, or early developmental periods[32]. Astroglial cells express ERα[33], ERβ[34], and G-protein coupled ERs[35], and although the full extent of ER functionality in astroglial cells is not understood[36], astroglia show rapid responses to hormones across various states and manipulations[37].

Because astroglial cells contribute to cortical development through neuroblast migration, neuronal network integration, and synapse formation, maturation and elimination, and because astroglia show rapid responses to hormones, we hypothesized that cortical astroglial cells may 1) show phenotypic sex differences both overall and across development and 2) execute developmental functions in a sexually dimorphic way. To address this, we employed a transgenic mouse model expressing enhanced green fluorescent protein (eGFP) fused to the L10 ribosome under the pan-astroglial cell promoter AldH-L1 and used immunohistochemistry and TRAPseq to phenotype the astroglial translatome and protein expression. We examined time points pertaining to critical periods of postnatal neocortical development.

Results

To measure total numbers of neocortical astroglial cells (astroglial cell number) across development, we used unbiased stereology to quantify eGFP+ cells (eGFP was expressed under the control of the pan-astroglial promoter, (AldH-L1). No sex differences in total astroglial number were observed ($F=0.716_{2,41}$, $p=0.402$, $H\eta=0.017$) (Figure 1A), however there was a main effect of age on this measure ($F=58.313_{2,41}$, $p<0.001$, $H\eta=0.874$), whereby the number of astroglial cells did not show further increase in males or females after P14 (Figure 1A). Neocortical volume did not exhibit sexual dimorphism ($F=0.009_{2,41}$, $p=0.923$, $H\eta=0$) (Figure 1B). Not surprisingly, we observed a significant increase of brain volume with age ($F=135.181_{2,41}$, $p<0.001$, $H\eta=0.943$) (Figure 1B).

Astroglial cell phenotype was assessed by looking at protein expression of common astroglial markers and characterising morphology. Astroglial cells show morphological heterogeneity that is often associated with functionality (Sofroniew & Vinters, 2010). In order to assess changes in morphology across age and/or sex, eGFP+ cells were characterized as radial or non-radial based on the presence of a leading, radial process in the neocortex. No significant sex effects were found ($F=0.004_{2,41}$, $p=0.953$, $H\eta=0$), however there was a significant effect of age ($F=89.291_{2,41}$, $p<0.001$, $H\eta=0.916$) (Figure 1C). Nearly all (~95% in both males and females) astroglial cells in the neocortex at P1 exhibited radial morphology (Figure 1C). At P4, there was a marked decrease in the proportion of radial astroglial cells and most cells shifted to a non-radial morphology with no marked sex differences. By P7, only 5% of astroglial cells in males and 4% of astroglial cells in females exhibited a radial morphology and, as expected, from P14 onwards there were virtually no radial astroglial cells remaining in the neocortex (<1%) (Figure 1C). We quantified expression of the astroglia-specific cytoskeletal filament protein glial acidic fibrillary protein, (GFAP). GFAP expression was not sexually dimorphic across development ($F=1.259_{2,41}$, $p=0.268$, $H\eta=0.029$) however, there was a main effect of age ($F=32.271_{2,41}$, $p<0.001$, $H\eta=0.793$) (Figure 1D). The number of GFAP+ cells reached peak levels at P14 and remained stable at later timepoints (Figure 1D). Prior to P14, no more than 15% of eGFP+ cells co-expressed GFAP, from P14-onwards approximately 25% of eGFP+ cells expressed GFAP, consistent with previous work that

has demonstrated that a large proportion of cortical astroglia do not express GFAP under basal conditions (Simard et al., 2018).

Next, we quantified the number of cells that expressed vimentin, an intermediate filament protein associated with a stem-like radial sub-type of astroglial cells. A significant interaction of sex by age was found ($F=3.871_{2,41}$, $p=0.006$, $H\eta=0.321$) (Figure 1E), such that females showed significantly more vimentin+ cells compared with males at P7 ($t=3.41$, $p=0.011$) and males showed significantly more vimentin+ cells in adulthood ($t=3.895$, $p=0.005$) (Figure 1E,G). Because vimentin expression is associated with astroglial cell neurogenic and stem cell potential and because we observed sex differences in vimentin expression, we quantified the proportion of actively dividing eGFP+ cells across the postnatal period. Using a marker of active s-phase cell division, Ki67, we quantified the percent of Ki67+eGFP+ cells. Ki67 was present in less than 2% of the astroglial cell population throughout the postnatal period in both males and females (Figure 1F). There were no significant sex differences across development ($F=0.862_{2,41}$, $p=0.358$, $H\eta=0.021$) however there was a main effect of age ($F=26.799_{2,41}$, $p<0.001$, $H\eta=0.766$).

To generate a complete phenotype of astroglial cells across development by sex, we used TRAPseq to assess the astroglial translatome at each time point. All expressed genes can be found in our searchable database at (TBA). To validate our TRAPseq methodology, we used q-RT-PCR to compare the unbound fragment to it's bound counterpart on levels of two astroglial genes (*GFAP and Glul)* and two neuronal genes (*Rbfox3 and Pvalb*). As expected, we found a large increase in astroglial gene expression in the bound fragment and a large reduction in neuronal-specific gene expression, suggesting a successful immunoprecipitation of the astroglial translatome (Supplemental Figure 4). In order to further characterise astroglial-specific markers by sex and age, we plotted expression data for each of the top 20 genes expressed only in postnatal cortical astroglia from both the Cahoy dataset[32] and 28 genes from the Zhang dataset[38] that were non-overlapping (Figure 2, 3 &4). Interestingly, most astroglia-specific genes (24/48) are expressed at increase across development, for example *CYP4F14*, a Vitamin E hydoroxylase and *SLC39A12*, a zinc transporter involved in the pathophysiology of

schizophrenia[39] both have low expression levels early on and rise to adult levels at P14 (Figure 2). Only one astroglial gene goes down in expression over development, *Pla2g3,* a gene involved in oxidative stress that has been linked to Alzheimer's disease [40]. Figure 3 depicts the 15/48 astroglial genes that show stable expression over development and finally, Figure 4 depicts those genes (8/48) that show less than 1RPKM and therefore have consistent low expression over the entire developmental period assessed. Interestingly, we did not find any sex differences in astroglia specific genes.

Figure 5A shows the hierarchical organization of the astroglial translatomes by sample. Overall, the clustering shows a pattern of organization that is primarily affected by age, with P1, P4 and P7 (early) showing similar expression patterns and P14, P35 and adult mice (late) showing similar expression patterns that differ from the early timepoints. We manually sorted samples by sex and age and although some organization by sex is noted in Figure 5B, this is not as clearly demarcated as that observed by age. Indeed, when we collapsed gene expression levels across all time points, 30 genes were differentially expressed between female and males (Supplementary Data File 1) in total, suggesting little to no sex differences in cortical astroglia overall. Moreover, many of these sex differences in gene expression are for genes located on the sex chromosomes. These findings suggest that overall, the basal translatome of cortical astroglia is not sexually dimorphic and that there are two major cortical astroglial phenotypes across age: an early (P1-P7) and late (P14-adult) phenotype.

To further characterize the *"early"* and *"late"* phenotype observed in the astroglial cell translatome, we examined the number and proportion of up- and downregulated genes in the early versus late developmental phenotypes, both by sex and collapsed across sex (Figure 6A). The early versus late phenotype in males showed 6904 DEGs whereas the female early versus late phenotype had 8811 DEGs (full list of DEGs in Supplementary Data File 2). Interestingly, the proportion of up- or downregulated genes was similar, with males and females showing 75% and 68% of DEGs in the early versus late phenotype being upregulated, respectively. When we collapsed the DEGs across sex to generate a general astroglial cell early vs late phenotype, the number of DEGs reaches 9990, distribution of up- (69%) and downregulation (31%) (Figure 6A). This suggests that

the difference in the early and late developmental phenotype is not merely reflective of turning off developmental genes but rather is a combination of downregulating genes associated with early development and turning on genes associated with later development and early adulthood. To validate the early/late phenotype that we found using TRAPseq, we compared TRAP extracted RNA on six genes differentially expressed between the early and late timepoints, 3 associated with synapse/network maturation (*Gja1, Lynx1, Grin2c*) and three steroid hormone receptors (*Ar, Pgr, Esr1*). Each of these showed a similar pattern of results (Supplemental Figure 5), which is highlighted by the significant positive correlations shown in Supplemental Figure 6.

Some key DEGs stand out as they have not previously been functionally described in astroglial cells. In particular, *Trim67*, an important and evolutionarily preserved guidance cue for neurite outgrowth[41], is high in early development and, as expected, decreases with age. Additionally, *Ntng1*, codes for Netrin G1, another guidance cue that is paramount to developing neuroblasts, is higher during the "early" developmental phenotype in astroglial cells. Differential *Ntng1* expression appears when examining both the overall and the sex-specific early versus late astroglial cell phenotype. *Ntng1* has been implicated in the etiology of familial schizophrenia[42] and *Ntng1* mRNA is in lower cortical samples from individuals with schizophrenia and autism[43].

Next, we compared the proportion of overlap between the female-specific and male-specific DEGs in the early versus late phenotype, and a clear sex difference emerges in the developmental expression pattern of astroglia. Of the 9602 unique DEGs, approximately 64% overlap between males and females, however about 28% of total DEGs are specific to females and only about 8% are specific to males (Figure 6B). This suggests that there are distinct developmental phenotypes in cortical astroglial cells that emerge between the sexes. When we further characterize the sex-specific canonical pathways (CPs) and gene ontology (GO) by gene set over-representation, a large proportion of the top five female-specific CPs are related to cell cycle/mitosis, marked by CPs related to mRNA processing and translation/ribosome function (Figure 6C). In comparison, male-specific CPs are related to oxidative phosphorylation and respiration (Figure 6C). With respect to GO, a large proportion of the top five female-specific GOs

are related to intracellular parts and organelles, whereas male-specific GO are related to mitochondrial protein and membrane organelles (Figure 6D).

To broaden the understanding of sex differences in astroglial cell gene expression across development, we identified DEGs of females versus males at each time point (Figure 7A). At P1, there are only 35 DEGs however at P7, P14, and P35 there are 129, 34 and 143 DEGs, respectively (Figure 7A; full list of DEGs in Supplementary Data File 1). In Figure 7B we show the number of DEGs between developmental time points in males and females, with a peak occurring between P7-14 in both females and males, with about 680 DEGs for males and 3136 for females. These sex differences between P7-P14 are particularly striking given that these are the developmental timepoints where sex hormones are largely dormant (Figure 7D; full list of DEGs in Supplementary Data File 3). This suggests that these sex differences in astroglial gene expression are part of a developmental program induced by sexually dimorphic perinatal exposure to hormones or by sex-linked chromosomes. Remarkably at P7, P14, and P35, 46%, 56%, and 99% of DEGs are downregulated in females. Within these downregulated genes are typical markers of cell activity, *Fos* and *Arc*, suggesting decreased basal activity in female astroglial cells at these timepoints (Supplementary Data File 1).

Work from the McCarthy laboratory has previously demonstrated that prostaglandins, and in particular, glial release of cyclooxengase 2 (COX-2) is a key regulator of estrogen-mediated architectural sex differences in the hypothalamus and the amygdala[44,45]. The gene for COX2, *Ptgs2*, is a sex-specific DEG in our data set in the overall females versus males, in the early female versus male phenotype, and at P1 female versus male (Supplementary Data File 1 & 2). To validate COX2 expression over development, we counted the number of cortical COX2+ cells co-localised with eGFP and saw a similar pattern as with our TRAPseq, with a significant sex difference in expression at P1 ($F_{12.517}$ $p=0.017$, $H\eta=0.715$)) (Figure 7C). COX2-mediated masculinization of the hypothalamus occurs in response to estradiol, which is aromatised from the surge in testosterone in males that occurs perinatally in rodents (Figure 7D). This perinatal surge in testosterone has been linked to sexual differentiation of the hypothalamus, amygdala, and mediates sexually dimorphic juvenile and adult behaviours[46-48]. To validate our

findings and to test if COX2 protein levels are similarly regulated by estrogen in the cortex, we subjected P0 females to estradiol benzoate injections and sacrificed them 36 hours later. The overall one-way ANOVA showed a trend for significance ($F=2.781_{3,20}$, $p=0.068$, $H\eta=0.294$), however because our previous experiment showed a difference between males and females, we conducted a planned comparison of these groups. Females at P1 show fewer COX2+ cells in the frontal cortex compared to males ($F=7.827_{1,9}$, $p=0.021$, $H\eta=0.465$) and females exposed to estrogen ($F=5.759_{1,9}$, $p=0.04$, $H\eta=0.390$) (Figure 7E). This suggests that estrogen exposure at P0 is sufficient to masculinize COX2 expression the cortex.

Next, we integrated the different altered gene sets in a coherent, systems-level context, using co-expression network analysis (see Online Methods). We inferred, (separately) a co-expression network in females and males throughout development, and identified 14 “female” and 17 “male” co-expression modules, including one unassigned gene module, grey. We then characterized the modules in terms of overlap with the DEGs in the early vs. late phenotype, correlation with developmental time point, and enrichment in GO terms and canonical pathways.

In females, the blue, yellow, and brown modules are enriched in genes upregulated in early vs. late , and the turquoise, magenta, green and pink modules are enriched in genes downregulated in early vs. late (see WGCNA Summary data). Interestingly, the blue, yellow and brown (upregulated) modules are enriched in astroglial genes. The turquoise module (downregulated) is enriched in cell cycle terms, and the green module (downregulated) is enriched in genes involved in translation, probably in relationship to cell cycle.

In the males’ network, the black, blue, brown, magenta, lightcyan, midnightblue and salmon modules are enriched in genes upregulated in early vs. late , and the green, red, yellow and turquoise modules are enriched in genes downregulated in early vs. late in males (see Supplementary File WGCNA). Similar to what was observed in the female network, some of the modules enriched in upregulated genes in the early vs. late phenotype in males (black, blue, brown and magenta), are enriched in astrocyte genes. It is likely that, in both networks, the astrocyte signature for the modules enriched in

upregulated genes reflects a shift in astroglial phenotype during development. Finally, the turquoise module (downregulated) is enriched in cell cycle terms, the green module (downregulated) is enriched in genes involved in translation, and the yellow module is enriched in genes involved in protein processing and cell cycle. The cell cycle signature for some of the downregulated modules likely reflects a reduction of proliferative potential of the cells over time, as would be expected over development.

Next, we tested each network, female and male, for enrichment in DEGs related to the opposite sex, to identify differentially enriched modules that might point to sex-specific modules, and, potentially to sex-specific regulation processes. In the female network, we found that the salmon and the green modules, are enriched in DEGs, respectively, upregulated and downregulated, in the early vs. late phenotype in females (i.e. downregulated in early vs late), but not in males. Further annotation of the salmon and green modules highlights enrichment in genes, respectively, upregulated and downregulated, after treatment with 17B–estradiol in the mouse (E2) (EnrichR: Ligand perturbation from GEO up/down).

In the male network, we found that the magenta module is enriched in DEGs upregulated in early vs. late phenotype in males, but not in females. Further annotation of the magenta module highlights, of relevance, enrichment in genes upregulated after treatment with 17B–estradiol in the mouse (E2) (EnrichR: Ligand perturbation from GEO up).

We next conducted an eigengene analysis where we plotted modules against age to evaluate how these modules changed over development and between males and females. We found consistent results across males and females whereby modules enriched with astroglial genes were increased over development, modules enriched with genes involved in cell cycle regulation were downregulated over development, modules involved in translation (ribosomes) were also downregulated and finally modules enriched in genes related to mitochondria and mitochondrial function were increased with age (Figure 8).

We next used a contingency table to contrast the modular organization of the two networks to assess the degree of correspondence, or the lack thereof, between them (see

Supplemental Figure 7). The contingency table reports the number of genes that fall into modules of the male network (rows) versus modules of the female network (columns). The table is color-coded by the ($-\log_{10}$) Fisher's exact test corrected p-value, to attach a significance level to each module overlap. Overall, the table shows good overlap between the two network modules, with each module in one network overlapping significantly with one or more modules of the other network. A few modules in the male network, pink, cyan, and magenta, show weak correspondence with the female network modules. This is interesting, since the pink and cyan modules are enriched in mitochondria genes and the magenta in astrocytes and lysosomes genes. And a single module in the female network, tan, shows weak correspondence to modules in the male network, however this module is not annotated. It should also be noted that overall module overlap does not imply similarity in structure, as the internal correlation structure may be different. Nevertheless, a module in one network that overlaps with multiple modules in the other network, may suggest potential differential regulation between the networks.

Discussion

In the current study, we generated a translatome database of cortical astroglial cells across development in both male and female mice. We show two clear astroglial phenotypes across development, an early (before P14) and late (after P14) phenotype. These early and late gene expression profiles reflect astroglia associated with early developmental functions related to gliogenesis and synaptogenesis and astroglia associated with functions involved in maturation, synapse elimination and maintaining a stable, homeostatic environment in adulthood (Figure 7D).

Surprisingly, cortical astroglial cells showed very little sexual dimorphism in either morphology or gene expression particularly in adulthood where very few DEGs were not sex-chromosome associated genes. Importantly, to assess basal differences between males and females in a conservative way, we chose to examine females during the metestrus phase, when ovarian hormones are at their lowest and therefore more similar to levels observed in males. As such, it is likely that greater sex differences in the astroglial translatome would be observed during other estrous cycle phases, such as in proestrus, when estrogen peaks. Indeed, we have previously demonstrated changes in cortical astroglial expression of GFAP and fibroblast growth factor 2 (FGF2), an astroglial mitogen and growth factor across the estrous cycle[49]. Together these results would suggest that astroglial cells show phenotypic changes in response to ovarian hormones, but they do not show basal sexual dimorphism.

Interestingly, the sex differences in DEGs observed at P7, 14, and 35 were not related to sex-specific canonical pathways or functions per se, but rather, they were related to general developmental phenomena such as cell cycle, and neuronal, dendritic and synaptic development, suggesting that astroglia modulate neuronal networks in a sexually dimorphic way. This could, in turn, potentially lead to the formation of sexually dimorphic neuronal networks, and presumably, sexually dimorphic behavioural expression later in life. Given the critical role of the neocortex in psychiatric disease and complex human behaviours[50], one might imagine that changes in neuronal network development may be induced by estrogen-modulated changes in astroglia. In addition, these may be particularly susceptible to developmental perturbations that modulate

hormone expression levels including exposure to stress hormones and environmental endocrine disruptors. Moreover, because hormone levels vary between individuals under normal conditions, this allows for a potential range of sexual differentiation of cortical networks, which would mirror behavioural sex differences observed across species, that are typically expressed on a continuum.

In contrast to the sex differences in gene expression seen on P7-P35, we see few DEGs between astroglia in male and female mice at P1, P4 and in adulthood. This, in addition to the sex differences in CP of early versus late astroglial phenotype, suggests that cortical astroglial cells employ different developmental strategies to reach a similar phenotype. The idea that distinct mechanisms might lead to similar functional results is similar to that put forward by Woolley[51], which was based on findings of estradiol potentiating glutamatergic synapses, albeit on a much more general level. Earlier DeVries[52] postulated that sex differences in gene expression patterns over development may actually prevent sex differences in specific regions or ensure that neuronal systems develop and are functional in the presence of cues such as sex hormones that are crucial for stimulating sex differences in target regions. It is possible that the sex differences in gene expression profiles between astroglia ensure that these systems develop “equally” in both sexes to achieve similar functionality in adulthood in the presence of sex chromosomes and hormones that are necessary to differentiate regions critical to sexually dimorphic behaviours, such as the hypothalamus.

The question remains as to what induces sex differences in cortical astroglia gene expression patterns over development. Three potential scenarios emerge: 1) sex chromosome-linked genes directly induce changes in gene expression patterns in astroglia. 2) The perinatal testosterone surge initiates cascades of gene expression patterns in astroglia that modulate cell maturation and network development. 3) Astroglial cells have a similar start and end point in our dataset. Given that sexual differentiation of the hypothalamus includes dramatic changes in neuronal number, arbours, and synapses on neurons that project to the neocortex, sex differences in astroglia gene expression could represent an active process to compensate for the sex differences in developing

neuronal inputs to the cortex. Importantly, these scenarios need not be mutually exclusive and may be active in parallel systems.

Scenario 1. Kdm5d appears as one of the few DEGs between females and males at P1 in our dataset, female expression levels are lower than males. *Kdm5d* is a Y-linked gene that encodes for demethylation enzymes and is required and sufficient to induce sexual differentiation of gene expression[53]. Indeed, changes in gene methylation may have profound effects that persist throughout time and cascades of gene expression may or may not be initiated, altering the responsiveness of the cell, and thus the network as a whole. Moreover, even in the absence of the testes determining *Sry* gene, the Y-chromosome has been shown to exert differential effects on developing peripheral and nervous tissue (reviewed in[54]), lending support to the idea that sex chromosome linked genes induce later sex differences in astroglia across development.

Scenario 2. Similarly, there is evidence that the perinatal testosterone surge, and consequentially, estrogen, is involved in the induction of developmental sex differences in astroglia. Our weighted network analysis shows enrichment of genes in several modules associated with responses to sex hormones and we show sex differences in the prostaglandin system (including Cox2) and that neonatal estrogen administration induces changes in cortical COX2 expression. Similar changes in astroglia have been demonstrated in the hypothalamus and are sufficient to produce observable sex differences in neuronal networks and associated behaviour[13]. Thus, the endogenous expression of estrogen early in development may facilitate a cascade of cellular maturation that in-turn will alter subsequent genetic programs. As such, the neuronal network will facilitate different programs as a result of the staggered pattern of maturation and communication.

Finally, *scenario 3* suggests that sex differences in the hypothalamus are necessary for a functional behavioural outcome that is overt and essential for sexual reproduction, first suggested by de Vries[52]. However, there are few overt measures that can be linked to cortical functioning that exhibit similar sexual dimorphisms, although sex differences in risk and resilience for psychiatric disease associated with cortical functioning are well-supported. For example, schizophrenia and ASD are more prominent

in the male population[8] and both show changes in developmental pathophysiology that occur both during the prenatal and postnatal periods[55,56]. There may be a relationship between astroglial neurogenic potential and the terminal phases of neuronal migration and construction and maturation of functional cortical networks that buffers females against developmental anomalies which, if left unchecked, may lead to schizophrenia or ASD morbidity.

In-line with this hypothesis, there are a number of models where estrogen treatment improves recovery or where females are protected in developmental injury models. Chronic postnatal hypoxia in rodents is used as a model of premature birth and induces loss of brain volume, particularly in the cortex and hippocampus, and leads to motor and cognitive impairments later in life[57,58]. The loss of cortical volume in the hypoxic model is less pronounced in females[57] and interestingly, estradiol treatment at the time of the injury improves white matter damage recovery[59]. It is also known that chronic postnatal hypoxia increases astroglial stem cell capacity[25,60]. This process may be enhanced in females allowing augmented recovery from the aversive effects of hypoxia, but may also speak to the nature of enhanced early postnatal plasticity in females compared to males. It is possible that females experience an enhanced or shifted neurogenic period early postnatally when we have observed an increase in vimentin+ astroglia that may translate to increased neurogenic potential of astroglial cells in the cortex. Similarly, while overt network or cellular sex differences may not modulate sex differences in risk for psychiatric disease, sex differences in developmental programs may leave one sex more vulnerable to perturbations during that time. Future studies will be needed to determine the functional significance of sex differences in developmental programs. Nevertheless, our data show a clear developmental pattern in cortical astroglia that differs between males and females, while no apparent basal sex differences in astroglia exist.

Online Methods

Animals

54 male and female C57/Bl6-AldHl1-L10-GFP transgenic mice generated from our breeding colony maintained at the Carleton University animal facility within the University of Ottawa. Mice were genotyped as in (Simard et al., 2018) and sex was determined by the presence or absence of tissues in the urogenital tract and confirmed by genotyping for the *Zfy* gene. All animals were group-housed until sacrifice in standard (27cm x 21cm x 14cm), fully transparent polypropylene cages with chew block, bedding, house and *ad libitum* access to standard lab chow (2014 Teklad Global 14% protein®) and water. Animals were raised in the standard environment with no outside manipulation except for standard care and to monitor estrous cycle stage (when applicable). The mice were maintained on a 12-hour light/dark cycle in a temperature controlled (21 degrees) facility. All animal use procedures have been approved by the Carleton University Committee for Animal Care, according to the guidelines set by the Canadian Council for the Use and Care of Animals in Research. Mice were overdosed and perfused for immunohistochemistry or rapidly decapitated for TRAPseq processing each on postnatal day 1* (P1) (36 hours postnatal), P4, P7, P14, P35 and adulthood (defined as 7-9 weeks of age) at the same time of day. Developmental time points and subject numbers are summarized in Supplementary Figure 1.

Organizational hormones study- 5 pregnant dams were ordered from Charles River and arrived at the Carleton University animal facility at the University of Ottawa at gestational day 15/16 and given 3 days to acclimatize to the environment. Dams were monitored intermittently overnight starting on gestational day 19 using red light. 31 male and female pups were randomly assigned to control or treatment groups approximately 1 hour following birth and sacrificed 35 hours later. The majority of groups in all experiments were formed with subjects from 3-5 separate litters to control for litter effects.

Estrous Cycle Monitoring

All adult group female animals were monitored daily after P35 to identify stage of estrous cycle using a saline lubricated swab inserted into the opening of the vagina to collect cells from the vaginal wall. Samples were smeared on a glass microscope slide

and examined under a 10x objective using a light microscope (VistaVision™). To understand basal organizational sex differences in astroglia, we used female mice in the phase of the estrous cycle with the lowest circulating ovarian hormones that has the least effect on cortical astroglial morphology and protein expression: metestrus[61]. After the stage of estrous cycle (Metestrus, Diestrus, Proestrus and Estrus) had been established for at least two full cycles, females were sacrificed during the light cycle of the metestrus stage.

Organizational hormones-injections

Estradiol benzoate (Chem Cruze, sc-205314) was dissolved in peanut oil (0.8g/mL) as per Hisasue et al., 2010 to allow for an injection of 20µg in a 25µL injection volume. Letrozole (Sigma-Aldrich, LG545-10MG) was dissolved in 0.3% hydroxypropyl cellulose PBS (Aldrich, 435007-5G) as per[62], to allow for an injection of 250mg/kg in a 25µL injection volume, sufficient to block all testosterone conversion based on average pup weight of 5g. Estradiol benzoate and letrozole solutions were prepared using glass materials and stored in a glass amber bottle to prevent absorption and disruption from plastics or ultraviolet exposure.

Animal Sacrifice

Rapid Decapitation for immunohistochemistry and qPCR- Animals in the P1 immunohistochemical group were rapidly decapitated and brains immediately placed in a 4% paraformaldehyde (Fisher Scientific) (PFA) solution at 4 ºC for 24h after which the brains were switched to 30% sucrose at 4 ºC for 24h. Following this period, brains were flash frozen until slicing. For the organizational hormone experiment, pups underwent rapid decapitation 36h following treatment. Brains were harvested and split along the central fissure. One hemisphere was flash frozen at -80°C for analysis in qPCR and the other hemisphere was fixed as above.

Cardiac Perfusion for Immunohistochemical Analysis- All mice were sacrificed for tissue collection at the same time of day during the light cycle. All mice in the immunohistochemical group underwent cardiac perfusion aside from those in group P1 (see above). Animals in P4, P7, P14, P35 and adult groups were given an overdose of 44mg/kg sodium pentobarbital (CDMV Canada), followed by intra-cardiac perfusion upon all spinal reflex cessation. Animals from the P4 and P7 groups underwent manual cardiac perfusion with 1mL of saline solution before receiving 1mL of 4% PFA via syringe. Mice in the P14, P35, and adult groups blood were flushed using 10mL of saline through the left atrium followed by 20mL of 4% PFA to fix the tissue. Brains were extracted and placed into vials containing 4% PFA and stored at 4 ºC. Following a 24h period, brains were transferred to a 30% sucrose in PBS (Fisher Scientific) solution and placed at 4 ºC.

Tissue sectioning

Following sucrose treatment, all brains were then flash frozen at -80 ºC until sectioning on a Leica (Leica™ CM1900) cryostat (30µm thick). 15 sets of sagittal sister sections were adhered to electrostatic slides (Fisher Scientific™) in rotating order, each slide therefore contained a full representation of the brain for stereological analysis as per previous studies[60,63].

Immunohistochemistry

All immunohistochemical processes took place at room temperature (~21 ºC) as per our previous studies[25,60,64]. One representative slide was taken from every subject and all subjects were processed simultaneously. Brain tissue from all groups were

prepared for immunohistochemistry using a 10% horse serum (Gibco™) PBS-T (0.3% TritonX (Fisher Scientific)) pre-block solution for 1 hour before being incubated with the respective primary antibody solution (see Supplementary Figure 1). Primary antibodies were diluted in 10% horse serum PBS-T (0.3% TritonX). Following approximately twenty-four hours of primary antibody incubation, slices were washed in a 1x PBS solution 3 times to remove unbound antibodies before being incubated with the species-appropriate fluorescein conjugated secondary antibody for visualization. Secondary antibodies were diluted in 10% horse serum PBS-T (0.3% TritonX) and incubated for 2 hours before slides were submerged in a 1x PBS wash 3 times to remove unbound antibodies. Slides were then coated with a nuclear stain, DAPI with hard setting mounting medium (VectorLabs), to fix glass cover slips and allowed to set before analysis. See Supplementary Figure 1 for antibodies and dilutions used.

Stereological Analysis

Unbiased estimates of cell numbers were obtained through use of Zeiss AxioImager M2 with ApoTome motorized fluorescent microscope (Carl Zeiss, Thornwood, NY, USA) in conjunction with a motorized stage and a computer running on Windows 7 using the program StereoInvestigator™ (MicroBrightfield, Colchester, VT, USA). Serial sagittal sections of the right hemisphere obtained through cryosectioning at 30µm on 15 sister sections were used for stereological analysis. Contours encompassing the whole right hemisphere neocortex on each section were drawn as boundaries in StereoInvestigator™. Cells were counted for expression of individual and/or co-expressed proteins using the optical fractionator probe at 40x. Sampling grids were optimized for cortical contours to include at minimum 3 sampling sites per contour to allow for a systematic and unbiased method to estimate cell density and cell quantification for right hemisphere of the cortex regardless of cell shape, size, orientation, spatial distribution, or post-mortem brain shrinkage[65]. Sampling boxes are randomly placed by StereoInvestigator™ within the sampling frame measuring 150µm x 150µm x 30µm with 3 of 6 exclusion borders. Total number of cells per count are reported via StereoInvestigator™ output. For analysis of astroglial morphology, StereoInvestigator™ (MBF, Vermont ™) software on a Zeiss Observer with Apotome (Zeiss™) was employed.

We identified and distinguished between radial and non-radial astroglial cells, counting these using unbiased sampling via the StereoInvestigator (MBF, Vermont ™) at 40x. Representative confocal mosaic images used for photomicrographs were taken using ZEN software (Zeiss™) with the Airyscan 800 microscope (Zeiss™).

TRAPseq

Translating ribosome affinity purification (TRAP)-sequencing was performed as per[66]. Briefly, eGFP-positive animals were rapidly decapitated and the brains removed and placed into a 1000x activated cyclohexamide (CHX) (100µg/ml, Sigma, dissolved in methanol, American Bioanalytical) dissection buffer at which point the cortex, removing any remaining white matter was dissected and flash-frozen in CHX dissection buffer at -80°C. When appropriate, brains were thawed on ice in homogenization buffer containing protease inhibitors, 1000x activated CHX, and RNAse inhibitors. Tissue samples were mechanically homogenized and then incubated on a rotisserie with anti-GFP (HtzGFP_04 (clone19F7) and HtzGFP_02 (clone 19C8): Memorial Sloan-Kettering Monoclonal Antibody Facility) coated biotinylated magnetic beads (Streptavidin MyOne T1 Dynabeads; Invitrogen # 65601) coated with Protein L (Fisher # PI-29997) at 4 ºC overnight. Following incubation with magnetic beads, the samples were collected on a magnet (DynaMag-2; Invitrogen #123-21D) and the unbound fragment was collected and frozen at -80 ºC. Bound mRNA fragments washed in polysome buffer underwent RNA extraction with DNAse treatment using Absolutely RNA Nanoprep Kit (Stratagene #400753).

RNA samples were sent to the Yale K.E.C.K facility for sample QC as per Simard et al. 2018: RNA quality was determined using a nanodrop and RNA integrity was determined by running an Agilent Bioanalyzer gel (RINs >8). mRNA was purified from approximately 500ng of total RNA with oligo-dT beads and sheared by incubation at 94C. Following first-strand synthesis with random primers, second strand synthesis was performed with dUTP for generating strand-specific sequencing libraries. The cDNA library was then end-repaired and A-tailed, adapters were ligated and second-strand digestion was performed by Uricil-DNA-Glycosylase. Indexed libraries that met appropriate cut-offs for both were quantified by qRT-PCR using a commercially available

kit: Kapa Library Quant Kit (Illumina) (KAPA Biosystems # KK4854-07960298001) and insert size distribution was determined with the LabChip GX or Agilent Bioanalyzer. Only samples with a yield of ≥0.5 ng/ul were used for sequencing.

Sample concentrations were normalized to 10 nM and loaded onto Illumina Rapid or High-output flow cells at a concentration that yields 130-250 million passing filter clusters per lane. Samples were sequenced using 75bp paired-end sequencing on an Illumina HiSeq 2500 according to Illumina protocols. The 6bp index was read during an additional sequencing read that automatically follows the completion of read 1. Data generated during sequencing runs were simultaneously transferred to the YCGA high-performance computing cluster. A positive control (prepared bacteriophage Phi X library) provided by Illumina is spiked into every lane at a concentration of 0.3% to monitor sequencing quality in real time.

Quantitative Real-Time PCR

To validate the enrichment of astroglial cell genes in our bound, immunoprecipitated fragment, the astroglial specific genes GFAP and Glul expression levels were compared between input and TRAP-immunoprecipitated fragments of one subject per each group (n=12). In addition, we evaluated RbFox3 and Pvalb gene expression assays to validate a concurrent decrease in neuronal gene expression. 20ng of RNA (concentration determined using NanoDrop (Thermofisher Scientific)) was used to produce cDNA using SuperScript IV First Strand Sythesis System (ThermoFisher Scientific). Best-coverage TAQMAN assays (Life Technologies) were run as per manufacturer's instructions and analyzed using the Applied Biosystems 7500 Real-Time PCR system and software.

To validate the TRAP-seq results we used RNA from all bound (*n*=55), immunoprecipitated fragments to produce cDNA using SuperScript III First-Strand Synthesis SuperMix (Thermo Fisher Scientific; catalog #11752050). We then performed a preamplification reaction (14 cycles) using TaqMan PreAmp Master Mix (Thermo Fisher Scientific; catalog #4384267), with a pooled-assay mix generated according to user guidelines. Finally, best-coverage TaqMan Gene Expression Assays (see Supp. Figure

3) were run as per the manufacturer's instructions using the Bio Rad CFX Connect Real Time system and software.

All CT values were obtained directly from the output generated by the software and delta delta CT's/fold change were calculated as per best practice guidelines [67].

Statistical Analysis

All immunohistochemical and qPCR data were analyzed for using a 2 (male vs. female) x 6 (P1 vs. P4 vs. P7 vs. P14 vs. P35 vs. Adult) between-subject factorial analyses of variance (ANOVA) design using IBM SPSS Statistics (Version 20.0). Because the treatment differed in males and females, for the organizational hormones study we employed a one-way ANOVA to determine overall significance. Post-hoc analysis using Bonferroni correction of pairwise comparisons for non-orthogonal comparisons were conducted when $p<0.05$. We re-ran all of the statistics including litter composition (male vs. female) as a covariate and found no significant effects of litter on any of the variables measured (data not shown).

RNAseq data analysis.

Sequencing reads were mapped to the mouse genome (GRCm38.p5) and the Ensembl (releas-84) transcriptome annotation, using HISAT2 [doi: 10.1038/nprot.2016.095]. The mapping rates ranged from 74% to 95%. This resulted in a number of mapped pairs from ~19.5 million up to 40 million (see Supplementary Table QC for more details). The resulting SAM files were converted to BAM formant using SAMtools[68]. FastQC v0.10.1 and RNA-SeQC (v1.1.8) were used for QC (see Supplemental Table QC). One male sample was excluded as it presented inconsistent read counts and had significant expression of male and female-specific genes including *Xist and ChrY* genes. The gene expression levels as counts were estimated using featureCounts[69] with the following options: -t exon; -g gene_id; -F "GTF"; -B; -s 0; -p; -a. Counts from technical replicates were added. Raw read counts were then filtered requiring more than 1 CPM (counts per million) in at least 25% of the samples and 16208 survived the filter and were considered for further analysis. We next used the sva

Bioconductor package [10.1093/bioinformatics/bts034] to identify and correct for latent variables. Hierarchical clustering (using the genes with a sd in expression level above the 95%) pre- and post sva correction show the sample-to-sample relationship and relative clustering (see Supplemental Figure 2). The edgeR function rpkm was used to estimate gene expression levels as RPKM.

Differential expression analysis. Differential expressed genes were then inferred using the edgeR pipeline[70], using the trended dispersion to estimate the biological variance and the GLM capability of the package. Nominal p-values from differential expression analysis were FDR corrected, and an FDR cut-off of 0.05 was used for all the tests.

Functional enrichment analysis. ConsensusPathDB[71] was used to test differentially expressed genes for overrepresentation in Gene Ontologies and Canonical Pathways.

Weighted gene co-expression network analysis. We used Weighted Gene Co-expression Network Analysis (WGCNA)[72] for co-expression network analysis using gene expression estimates (as log2(RPKM+1)), separately, from the 25 male samples and the 26 female samples, after cqn and sva correction. We estimated a male and female the co-expression network and modules using the function blockwiseModule, using the bicorr as correlation estimate, a “signed” network type and a minModuleSize=50. The power cut-off was set to 16 for both sets. The analysis produced a male network of 13 modules and a female network of 15 modules, including the grey module of unassigned genes (See WGCNA Summary Data).

Data Availibility

Data analyzed during this study are either included in this published article supplementary files, or available upon request. RNAseq data are accessible through our database (TBA) , or available from the GEO repository (accession number to be added)

Code availability

All the custom code used for processing RNAseq data is available upon request

References

1 Molyneaux, B. J., Arlotta, P., Menezes, J. R. L. & Macklis, J. D. Neuronal subtype specification in the cerebral cortex. *Nature Reviews Neuroscience* **8**, 427-437, doi:10.1038/nrn2151 (2007).

2 Barton, R. A. & Harvey, P. H. Mosaic evolution of brain structure in mammals. *Nature* **405**, 1055-1058, doi:10.1038/35016580 (2000).

3 Berry, M. & Rogers, A. W. The migration of neuroblasts in the developing cerebral cortex. *Journal of anatomy* **99**, 691-709 (1965).

4 Rakic, P. Mode of cell migration to the superficial layers of fetal monkey neocortex. *The Journal of Comparative Neurology* **145**, 61-83, doi:10.1002/cne.901450105 (1972).

5 Strakowski, S. M. *et al.* The functional neuroanatomy of bipolar disorder: a consensus model. *Bipolar Disorders* **14**, 313-325, doi:10.1111/j.1399-5618.2012.01022.x (2012).

6 Lin, C.-H. & Lane, H.-Y. Early Identification and Intervention of Schizophrenia: Insight From Hypotheses of Glutamate Dysfunction and Oxidative Stress. *Frontiers in psychiatry* **10**, 93, doi:10.3389/fpsyt.2019.00093 (2019).

7 Bayés, À. *et al.* Characterization of the proteome, diseases and evolution of the human postsynaptic density. *Nature Neuroscience* **14**, 19-21, doi:10.1038/nn.2719 (2011).

8 Bao, A.-M. & Swaab, D. F. Sexual differentiation of the human brain: Relation to gender identity, sexual orientation and neuropsychiatric disorders. *Frontiers in neuroendocrinology* **32**, 214-226, doi:10.1016/j.yfrne.2011.02.007 (2011).

9 Donner, N. C. & Lowry, C. A. Sex differences in anxiety and emotional behavior. *Pflugers Archiv : European journal of physiology* **465**, 601-626, doi:10.1007/s00424-013-1271-7 (2013).

10 Jaric, I., Rocks, D., Cham, H., Herchek, A. & Kundakovic, M. Sex and Estrous Cycle Effects on Anxiety- and Depression-Related Phenotypes in a Two-Hit Developmental Stress Model. *Frontiers in molecular neuroscience* **12**, 74, doi:10.3389/fnmol.2019.00074 (2019).

11 Kokras, N. *et al.* Forced swim test: What about females? *Neuropharmacology* **99**, 408-421, doi:10.1016/J.NEUROPHARM.2015.03.016 (2015).

12 McEwen, B. S., Lieberburg, I., Chaptal, C. & Krey, L. C. Aromatization: Important for sexual differentiation of the neonatal rat brain. *Hormones and Behavior* **9**, 249-263, doi:10.1016/0018-506X(77)90060-5 (1977).

13 Wright, C. L., Schwarz, J. S., Dean, S. L. & McCarthy, M. M. Cellular mechanisms of estradiol-mediated sexual differentiation of the brain. *Trends in Endocrinology & Metabolism* **21**, 553-561, doi:10.1016/j.tem.2010.05.004 (2010).

14 GORSKI, R. A. & WAGNER, J. W. Gonadal Activity and Sexual Differentiation of the Hypothalamus. *Endocrinology* **76**, 226-239, doi:10.1210/endo-76-2-226 (1965).

15 Johnson, R. T., Breedlove, S. M. & Jordan, C. L. Androgen receptors mediate masculinization of astrocytes in the rat posterodorsal medial amygdala during puberty. *The Journal of comparative neurology* **521**, 2298-2309, doi:10.1002/cne.23286 (2013).

16 Woolley, C. S., Gould, E., Frankfurt, M. & McEwen, B. S. Naturally occurring fluctuation in dendritic spine density on adult hippocampal pyramidal neurons. *Journal of Neuroscience* **10** (1990).

17 Bowers, J. M., Waddell, J. & Mccarthy, M. M. A developmental sex difference in hippocampal neurogenesis is mediated by endogenous oestradiol. *Biology of Sex Differences* **1**, 8, doi:10.1186/2042-6410-1-8 (2010).

18 Frazier, T. W., Georgiades, S., Bishop, S. L. & Hardan, A. Y. Behavioral and Cognitive Characteristics of Females and Males With Autism in the Simons Simplex Collection. *Journal of the American Academy of Child & Adolescent Psychiatry* **53**, 329-340.e323, doi:10.1016/J.JAAC.2013.12.004 (2014).

19 Parellada, M., Gomez-Vallejo, S., Burdeus, M. & Arango, C. Developmental Differences Between Schizophrenia and Bipolar Disorder. *Schizophrenia Bulletin* **43**, 1176-1189, doi:10.1093/schbul/sbx126 (2017).

20 Sloan, S. A. & Barres, B. A. Mechanisms of astrocyte development and their contributions to neurodevelopmental disorders. *Current opinion in neurobiology* **27**, 75-81, doi:10.1016/j.conb.2014.03.005 (2014).

21 Clarke, L. E. & Barres, B. A. Emerging roles of astrocytes in neural circuit development. *Nature Reviews Neuroscience* **14**, 311-321, doi:10.1038/nrn3484 (2013).

22 Loo, L. *et al.* Single-cell transcriptomic analysis of mouse neocortical development. *Nature communications* **10**, 134-134, doi:10.1038/s41467-018-08079-9 (2019).

23 Bayraktar, O. A. *et al.* Single-cell in situ transcriptomic map of astrocyte cortical layer diversity. *bioRxiv*, 432104, doi:10.1101/432104 (2018).

24 Anthony, T. E., Klein, C., Fishell, G. & Heintz, N. Radial Glia Serve as Neuronal Progenitors in All Regions of the Central Nervous System. *Neuron* **41**, 881-890, doi:10.1016/S0896-6273(04)00140-0 (2004).

25 Bi, B. *et al.* Cortical glial fibrillary acidic protein-positive cells generate neurons after perinatal hypoxic injury. *The Journal of neuroscience : the official journal of the Society for Neuroscience* **31**, 9205-9221, doi:10.1523/JNEUROSCI.0518-11.2011 (2011).

26 Ganat, Y. M. *et al.* Early Postnatal Astroglial Cells Produce Multilineage Precursors and Neural Stem Cells In Vivo. *Journal of Neuroscience* **26**, 8609-8621, doi:10.1523/JNEUROSCI.2532-06.2006 (2006).

27 Salmaso, N., Tomasi, S. & Vaccarino, F. M. Neurogenesis and maturation in neonatal brain injury. *Clinics in perinatology* **41**, 229-239, doi:10.1016/j.clp.2013.10.007 (2014).

28 Sofroniew, M. V. & Vinters, H. V. Astrocytes: biology and pathology. *Acta neuropathologica* **119**, 7-35, doi:10.1007/s00401-009-0619-8 (2010).

29 Chever, O., Pannasch, U., Ezan, P. & Rouach, N. Astroglial connexin 43 sustains glutamatergic synaptic efficacy. *Philosophical Transactions of the Royal Society of London B: Biological Sciences* **369** (2014).

30 Diniz, L. P. *et al.* Astrocyte transforming growth factor beta 1 promotes inhibitory synapse formation via CaM kinase II signaling. *Glia* **62**, 1917-1931, doi:10.1002/glia.22713 (2014).

31 Di Garbo, A., Barbi, M., Chillemi, S., Alloisio, S. & Nobile, M. Calcium signalling in astrocytes and modulation of neural activity. *Bio Systems* **89**, 74-83, doi:10.1016/j.biosystems.2006.05.013 (2007).

32 Cahoy, J. D. *et al.* A Transcriptome Database for Astrocytes, Neurons, and Oligodendrocytes: A New Resource for Understanding Brain Development and Function. *The Journal of Neuroscience* **28**, 264 LP-278, doi:10.1523/JNEUROSCI.4178-07.2008 (2008).

33 Milner, T. A. *et al.* Ultrastructural evidence that hippocampal alpha estrogen receptors are located at extranuclear sites. *Journal of Comparative Neurology* **429**, 355-371, doi:10.1002/1096-9861(20010115)429:3<355::AID-CNE1>3.0.CO;2-# 10.1002/1096-9861(20010115)429:33.0.CO;2-# (2001).

34 Platania, P. *et al.* Differential Expression of Estrogen Receptors Alpha and Beta in the Spinal Cord during Postnatal Development: Localization in Glial Cells. *Neuroendocrinology* **77**, 334-340, doi:10.1159/000070899 (2003).

35 Lee, E. *et al.* GPR30 regulates glutamate transporter GLT-1 expression in rat primary astrocytes. *The Journal of biological chemistry* **287**, 26817-26828, doi:10.1074/jbc.M112.341867 (2012).

36 Piechota, M. *et al.* Transcriptional signatures of steroid hormones in the striatal neurons and astrocytes. *BMC Neuroscience* **18**, 37, doi:10.1186/s12868-017-0352-5 (2017).

37 Acaz-Fonseca, E., Avila-Rodriguez, M., Garcia-Segura, L. M. & Barreto, G. E. Regulation of astroglia by gonadal steroid hormones under physiological and pathological conditions. *Progress in Neurobiology* **144**, 5-26, doi:10.1016/J.PNEUROBIO.2016.06.002 (2016).

38 Zhang, Y. *et al.* An RNA-sequencing transcriptome and splicing database of glia, neurons, and vascular cells of the cerebral cortex. *The Journal of neuroscience : the official journal of the Society for Neuroscience* **34**, 11929-11947, doi:10.1523/JNEUROSCI.1860-14.2014 (2014).

39 Scarr, E. *et al.* Increased cortical expression of the zinc transporter SLC39A12 suggests a breakdown in zinc cellular homeostasis as part of the pathophysiology of schizophrenia. *npj Schizophrenia* **2**, 16002, doi:10.1038/npjschz.2016.2 (2016).

40 Martinez-Garcia, A. *et al.* PLA2G3, a gene involved in oxidative stress induced death, is associated with Alzheimer's disease. *Journal of Alzheimer's disease : JAD* **22**, 1181-1187, doi:10.3233/jad-2010-101348 (2010).

41 Yaguchi, H. *et al.* TRIM67 protein negatively regulates Ras activity through degradation of 80K-H and induces neuritogenesis. *The Journal of biological chemistry* **287**, 12050-12059, doi:10.1074/jbc.M111.307678 (2012).

42 Aoki-Suzuki, M. *et al.* A family-based association study and gene expression analyses of netrin-G1 and -G2 genes in schizophrenia. *Biological psychiatry* **57**, 382-393, doi:10.1016/j.biopsych.2004.11.022 (2005).

43 Eastwood, S. L. & Harrison, P. J. Decreased mRNA expression of netrin-G1 and netrin-G2 in the temporal lobe in schizophrenia and bipolar disorder. *Neuropsychopharmacology : official publication of the American College of Neuropsychopharmacology* **33**, 933-945, doi:10.1038/sj.npp.1301457 (2008).

44 Bowers, J. M., Waddell, J. & McCarthy, M. M. A developmental sex difference in hippocampal neurogenesis is mediated by endogenous oestradiol. *Biology of Sex Differences* **1**, 8-8, doi:10.1186/2042-6410-1-8 (2010).

45 Lenz, K. M. & McCarthy, M. M. Organized for sex - steroid hormones and the developing hypothalamus. *The European journal of neuroscience* **32**, 2096-2104, doi:10.1111/j.1460-9568.2010.07511.x (2010).

46 Lenz, K. M. & McCarthy, M. M. Organized for sex - steroid hormones and the developing hypothalamus. *The European journal of neuroscience* **32**, 2096-2104, doi:10.1111/j.1460-9568.2010.07511.x (2010).

47 Clarkson, J. & Herbison, A. E. Hypothalamic control of the male neonatal testosterone surge. *Philosophical transactions of the Royal Society of London. Series B, Biological sciences* **371**, 20150115, doi:10.1098/rstb.2015.0115 (2016).

48 Swaab, D. F. Sexual differentiation of the brain and behavior. *Best Practice & Research Clinical Endocrinology & Metabolism* **21**, 431-444, doi:10.1016/j.beem.2007.04.003 (2007).

49 Salmaso, N. & Woodside, B. Fluctuations in astrocytic basic fibroblast growth factor in the cingulate cortex of cycling, ovariectomized and postpartum animals. *Neuroscience* **154**, 932-939, doi:10.1016/J.NEUROSCIENCE.2008.03.063 (2008).

50 Arnsten, A. F. T. Ameliorating prefrontal cortical dysfunction in mental illness: inhibition of phosphotidyl inositol-protein kinase C signaling. *Psychopharmacology* **202**, 445-455, doi:10.1007/s00213-008-1274-9 (2009).

51 Oberlander, J. G. & Woolley, C. S. 17β-Estradiol Acutely Potentiates Glutamatergic Synaptic Transmission in the Hippocampus through Distinct Mechanisms in Males and Females. *The Journal of neuroscience : the official journal of the Society for Neuroscience* **36**, 2677-2690, doi:10.1523/JNEUROSCI.4437-15.2016 (2016).

52 De Vries, G. J. Minireview: Sex Differences in Adult and Developing Brains: Compensation, Compensation, Compensation. *Endocrinology* **145**, 1063-1068, doi:10.1210/en.2003-1504 (2004).

53 Mizukami, H. *et al.* KDM5D-mediated H3K4 demethylation is required for sexually dimorphic gene expression in mouse embryonic fibroblasts. *The Journal of Biochemistry* **165**, 335-342, doi:10.1093/jb/mvy106 (2018).

54 Arnold, A. P. *et al.* Minireview: Sex Chromosomes and Brain Sexual Differentiation. *Endocrinology* **145**, 1057-1062, doi:10.1210/en.2003-1491 (2004).

55 Galvez-Contreras, A. Y., Campos-Ordonez, T., Gonzalez-Castaneda, R. E. & Gonzalez-Perez, O. Alterations of Growth Factors in Autism and Attention-Deficit/Hyperactivity Disorder. *Frontiers in psychiatry* **8**, 126, doi:10.3389/fpsyt.2017.00126 (2017).

56 Matute, C., Melone, M., Vallejo-Illarramendi, A. & Conti, F. Increased expression of the astrocytic glutamate transporter GLT-1 in the prefrontal cortex of schizophrenics. *Glia* **49**, 451-455, doi:10.1002/glia.20119 (2005).

57 Mayoral, S. R., Omar, G. & Penn, A. A. Sex differences in a hypoxia model of preterm brain damage. *Pediatric research* **66**, 248-253, doi:10.1203/PDR.0b013e3181b1bc34 (2009).

58 van der Kooij, M. A. *et al.* Mild neonatal hypoxia–ischemia induces long-term motor- and cognitive impairments in mice. *Brain, Behavior, and Immunity* **24**, 850-856, doi:https://doi.org/10.1016/j.bbi.2009.09.003 (2010).

59 Gerstner, B. *et al.* 17beta-estradiol protects against hypoxic/ischemic white matter damage in the neonatal rat brain. *Journal of neuroscience research* **87**, 2078-2086, doi:10.1002/jnr.22023 (2009).

60 Salmaso, N. *et al.* Environmental enrichment increases the GFAP+ stem cell pool and reverses hypoxia-induced cognitive deficits in juvenile mice. *The Journal of neuroscience : the official journal of the Society for Neuroscience* **32**, 8930-8939, doi:10.1523/JNEUROSCI.1398-12.2012 (2012).

61 Gillies, G. E. & McArthur, S. Estrogen actions in the brain and the basis for differential action in men and women: a case for sex-specific medicines. *Pharmacological reviews* **62**, 155-198, doi:10.1124/pr.109.002071 (2010).

62 Bowen, R. S., Ferguson, D. P. & Lightfoot, J. T. Effects of Aromatase Inhibition on the Physical Activity Levels of Male Mice. *Journal of steroids & hormonal science* **1**, 1-7, doi:10.4172/2157-7536.S1-001 (2011).

63 Komitova, M. *et al.* Hypoxia-induced developmental delays of inhibitory interneurons are reversed by environmental enrichment in the postnatal mouse forebrain. *The Journal of neuroscience : the official journal of the Society for Neuroscience* **33**, 13375-13387, doi:10.1523/JNEUROSCI.5286-12.2013 (2013).

64 Salmaso, N. *et al.* Contribution of maternal oxygenic state to the effects of chronic postnatal hypoxia on mouse body and brain development. *Neuroscience letters* **604**, 12-17, doi:10.1016/j.neulet.2015.07.033 (2015).

65 Schmitz, C. & Hof, P. R. Design-based stereology in neuroscience. *Neuroscience* **130**, 813-831, doi:10.1016/j.neuroscience.2004.08.050 (2005).

66 Simard, S. *et al.* Profiling changes in cortical astroglial cells following chronic stress. *Neuropsychopharmacology : official publication of the American College of Neuropsychopharmacology* **43**, 1961-1971, doi:10.1038/s41386-018-0105-x (2018).

67 Bustin, S. A. *et al.* The MIQE guidelines: minimum information for publication of quantitative real-time PCR experiments. *Clinical chemistry* **55**, 611-622, doi:10.1373/clinchem.2008.112797 (2009).

68 Li, H. *et al.* The Sequence Alignment/Map format and SAMtools. *Bioinformatics (Oxford, England)* **25**, 2078-2079, doi:10.1093/bioinformatics/btp352 (2009).

69 Liao, Y., Smyth, G. K. & Shi, W. featureCounts: an efficient general purpose program for assigning sequence reads to genomic features. *Bioinformatics (Oxford, England)* **30**, 923-930, doi:10.1093/bioinformatics/btt656 (2014).

70 Robinson, M. D., McCarthy, D. J. & Smyth, G. K. edgeR: a Bioconductor package for differential expression analysis of digital gene expression data. *Bioinformatics (Oxford, England)* **26**, 139-140, doi:10.1093/bioinformatics/btp616 (2010).

71 Kamburov, A., Stelzl, U., Lehrach, H. & Herwig, R. The ConsensusPathDB interaction database: 2013 update. *Nucleic acids research* **41**, D793-800, doi:10.1093/nar/gks1055 (2013).

72 Langfelder, P. & Horvath, S. WGCNA: an R package for weighted correlation network analysis. *BMC Bioinformatics* **9**, 559-559, doi:10.1186/1471-2105-9-559 (2008).

Figure Captions

Figure 1. A- Total number of eGFP+ cells in the neocortex. B- Estimated neocortical volume. C- Percentage of radial-like eGFP+ cells. D- Total number of cells expressing GFAP. E- Total number of vimentin+ cells. F- Percent GFP+ coexpressing Ki67. G- Representative mosaic of confocal pictomicrographs at 10x, whole cortex sagittal section (left), zoom on the molecular layer (right). * indicates a significant difference from all other time points; # indicates a significant difference between male and female at that time point. Bars denote group mean and error bars displayed are ± SEM.

Figure 2. Average expression levels (RPKM) of astroglial-specific genes as identified in Cahoy et al., 2008 and Zhang et al., 2014 that increase or decrease across examined timepoints. Error bars are displayed as ± SEM.

Figure 3. Average expression levels (RPKM) of astroglial-specific genes as identified in Cahoy et al., 2008 and Zhang et al., 2014 that remain stable (Log2fold change<2) across examined time points. Error bars are displayed as ± SEM.

Figure 4. Average expression levels (RPKM) of astroglial-specific genes as identified in Cahoy et al., 2008 and Zhang et al., 2014 that have less than 1RPKMs across examined time points. Error bars are displayed as ± SEM.

Figure 4. A- Clustered heat map of individual sample gene expression levels from TRAPseq data. B- Represents a heat map of samples manually sorted by sex and age.

Figure 6. A- Number of DEGs between early and late phenotype in males and females. B- Venn diagram displaying overlap in DEGs between females and males. Overlapping gene lists were generated using GeneVenn supported by the University of Southern Mississippi. C- Canonical pathways (CPs) for males right (bordered by blue), and females left (bordered by red). D- Geneontology (GO) for males right (bordered by blue), and females left (bordered by red). CPs and GO were generated with the Consensus Path Database-Mouse version MM10 (01-01-2019) supported by the Max Planck Institute for Molecular Genetics using gene set analysis, over-representation analysis. Pathways and gene ontology generated using “pathways database” and “gene ontology level 2” using the top 5 called pathways for male and female-specific DEGs from early versus late phenotypes.

Figure 7. A- Graphical representation of number of up- and downregulated DEGs between males and females at each time point. B- Graphical representation of DEGs between time points. C- Density of COX2+ cells in the cortex across examined timepoints. Bars represent group means, error bars are displayed as ± SEM. Representative mosaic reconstruction of Cox2, eGFP staining in a male and female mouse within the PFC region of the cortex at P1 (top). A 63X+oil image highlighting a Cox2+, eGFP+ astroglia (white arrow) and a Cox2-, eGFP+ astroglia (pink arrow) in the

PFC (bottom). D, top panel- Graphical illustration of arbitrary levels circulating gonadal hormones (testosterone, solid lines; estrogen, broken lines) in males (blue) and females (red) overlay with ages examined in the study. D, lower panel- important cortical neurulation events represented by colour saturation. Darker saturation indicates when a process is more active, lower saturation indicates when a process is less active. (Adapted from: Ellis 2004; Gillies and McArthur, 2010; Anderson, 2003; Estes and McAllistter, 2016). E- Density of COX2+ cells in the cortex at P1 in males and females treated with estradiol or letrozole. Bars represent group means, error bars are displayed as ± SEM.

Figure 8- Eigengene analysis of WGCNA-identified modules. Plots depict module expression levels against age in males and females, subdivided by the module annotation.

Figure 1

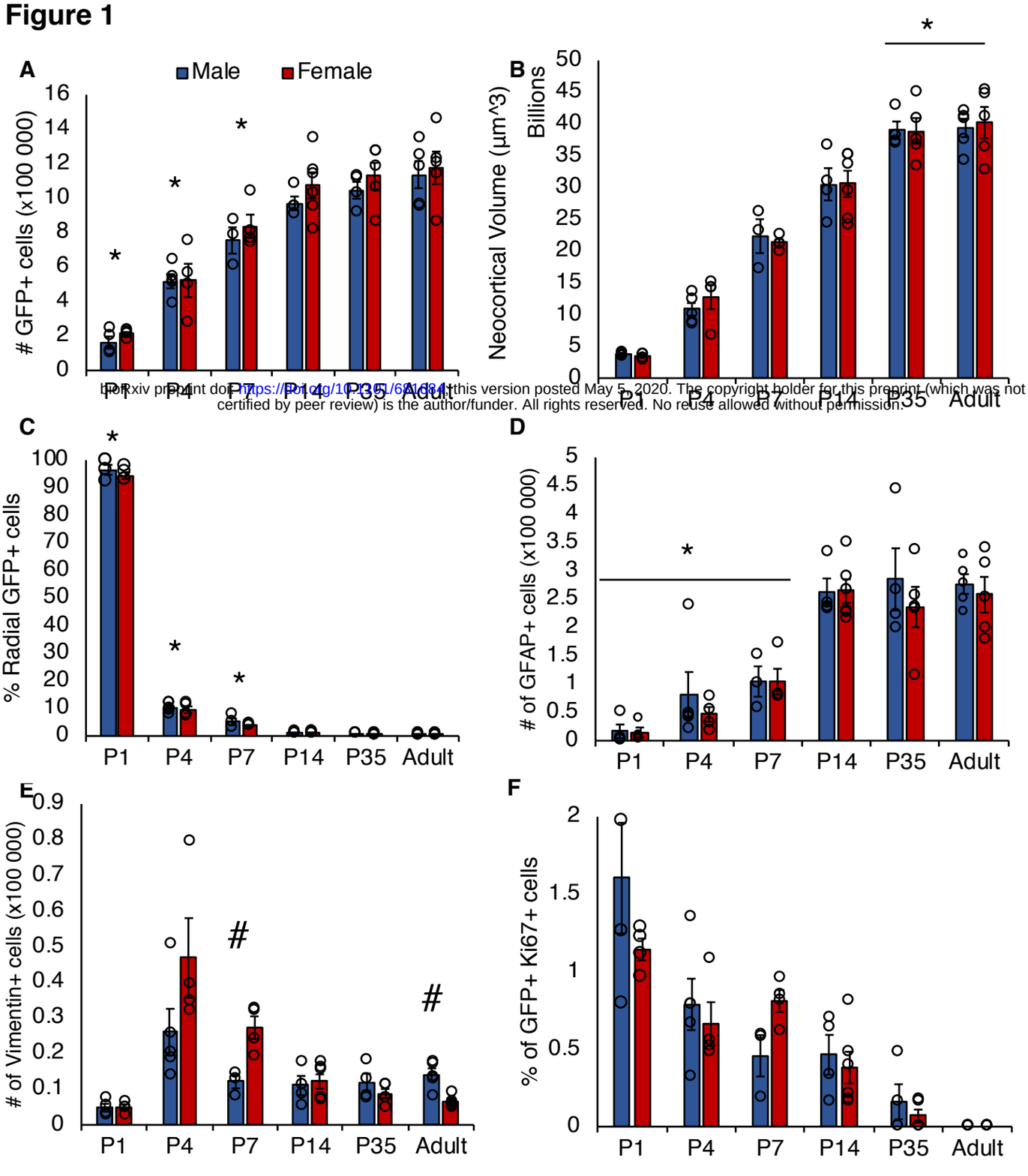

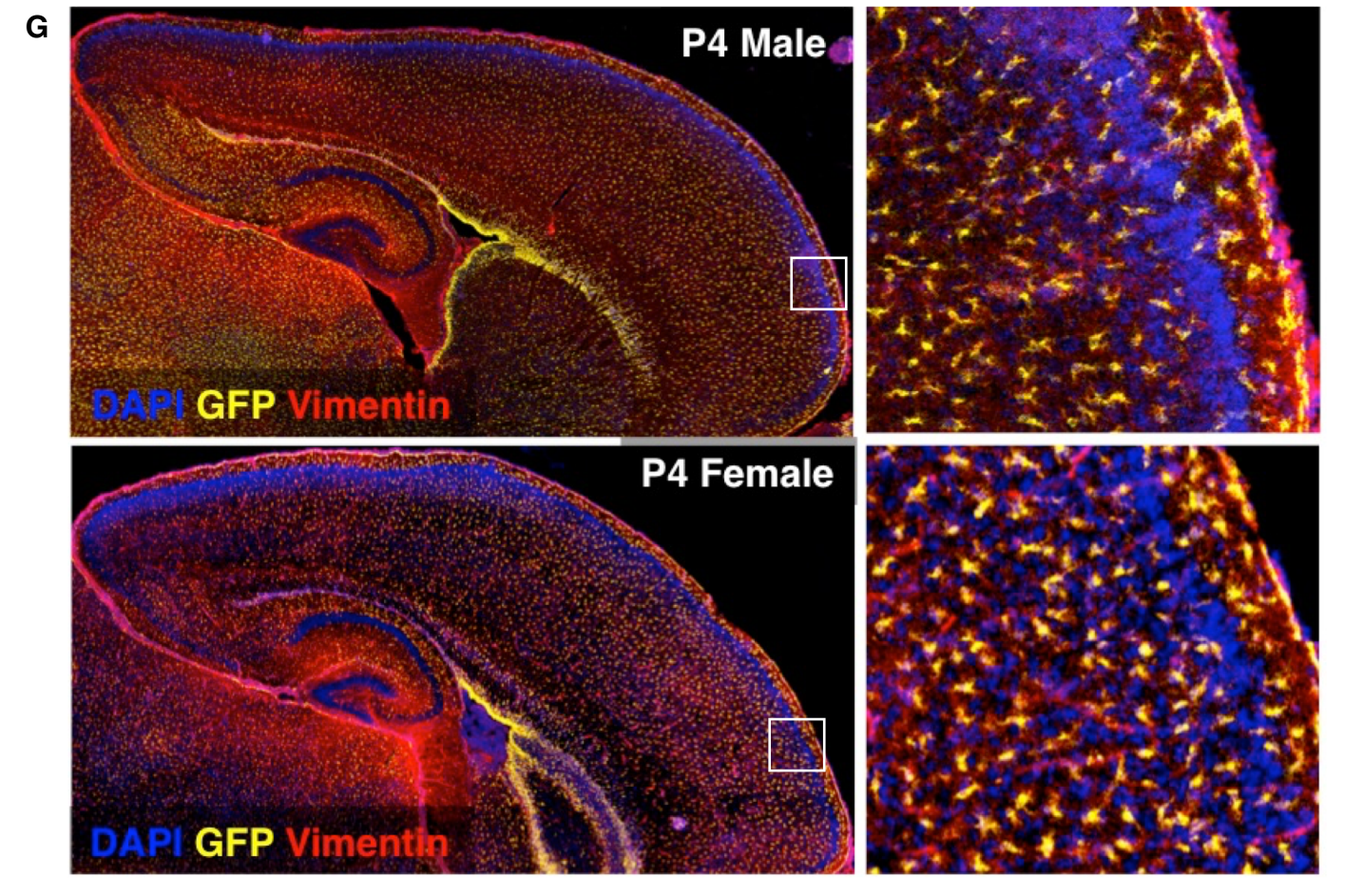

Figure 2

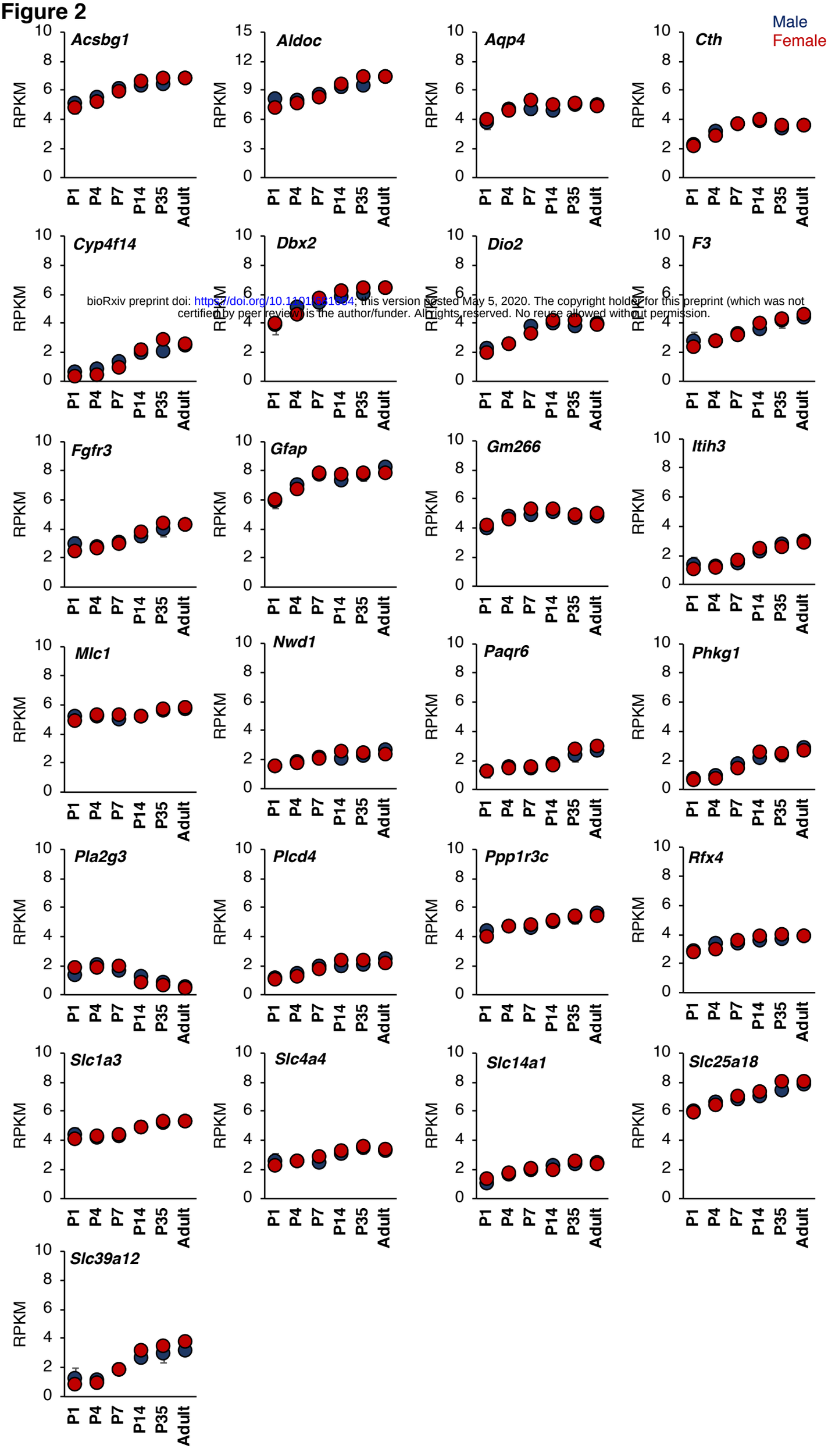

Figure 3

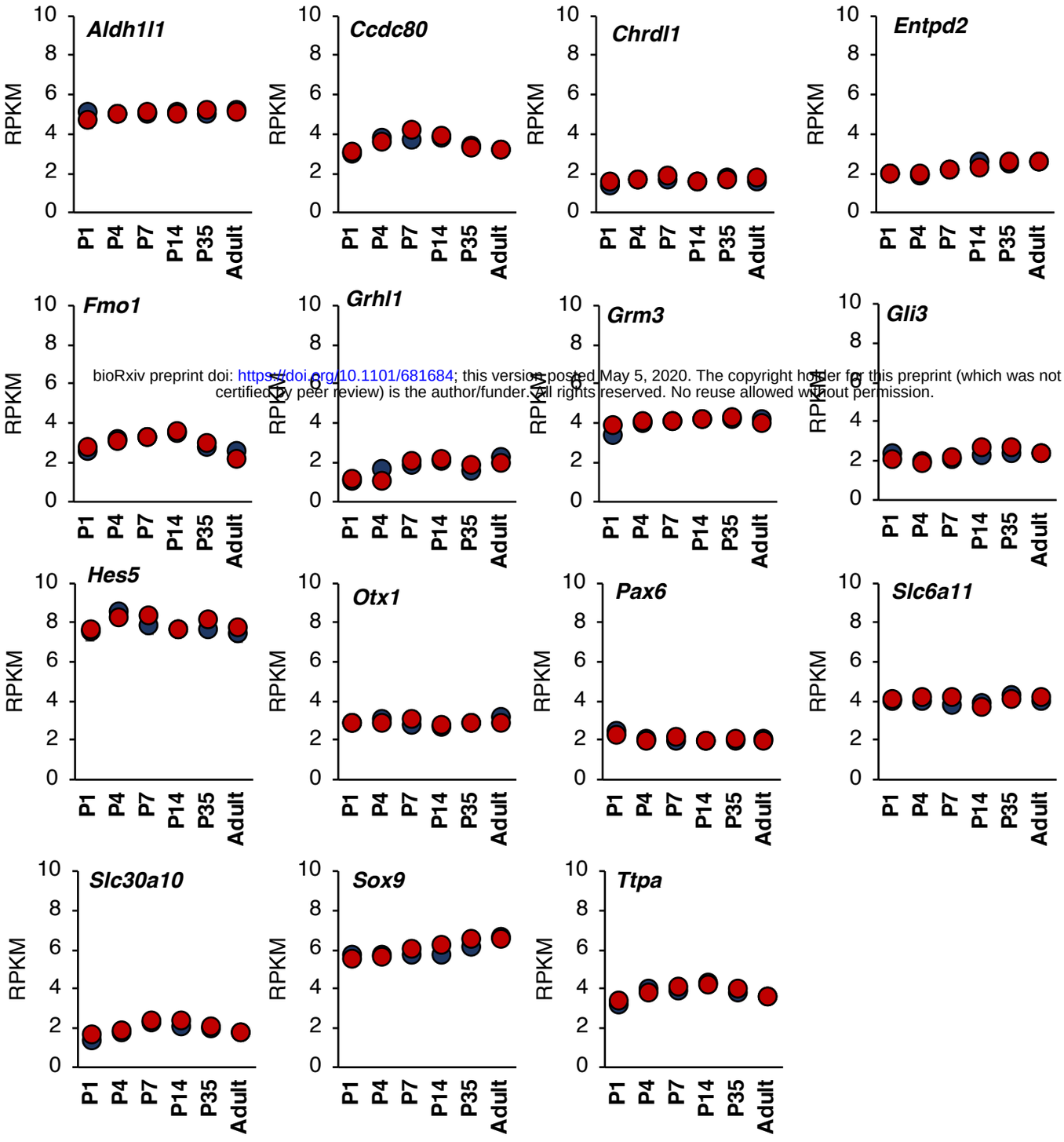

Figure 4

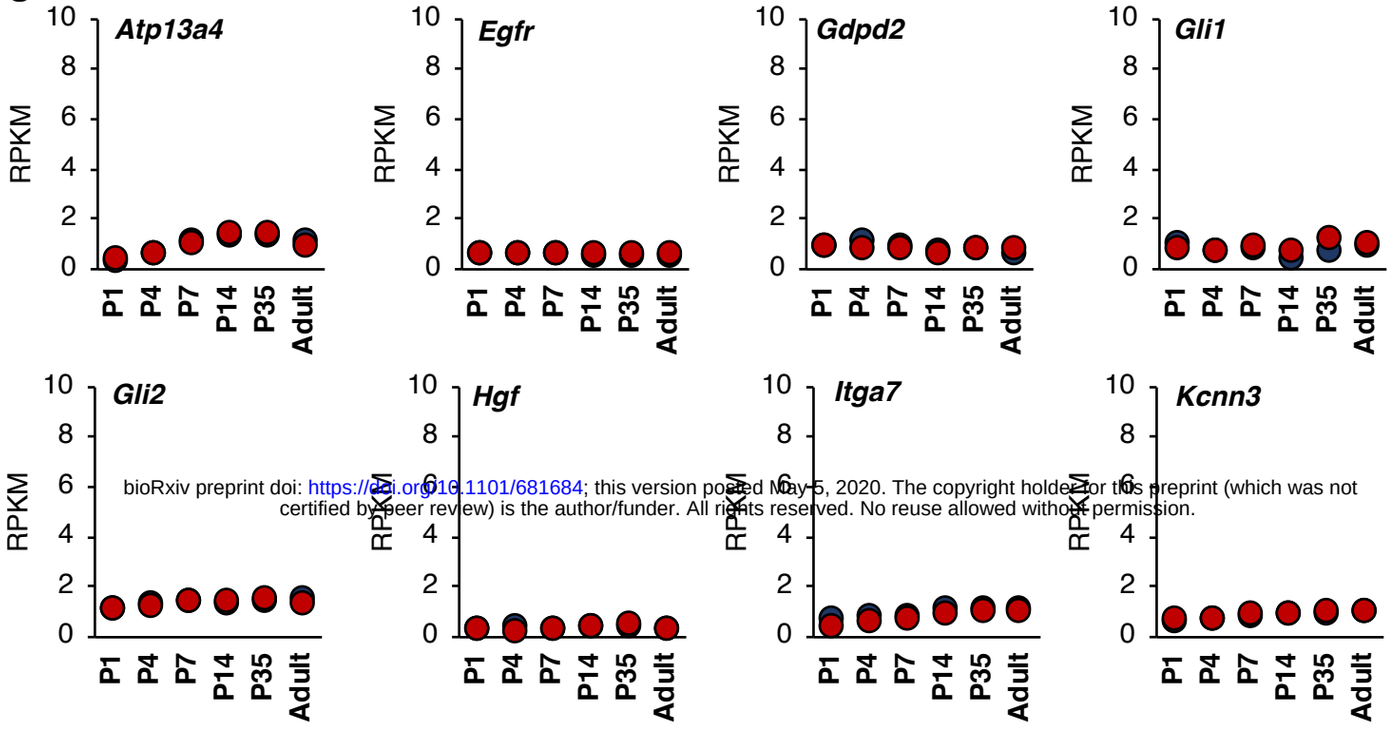

Figure 5

A

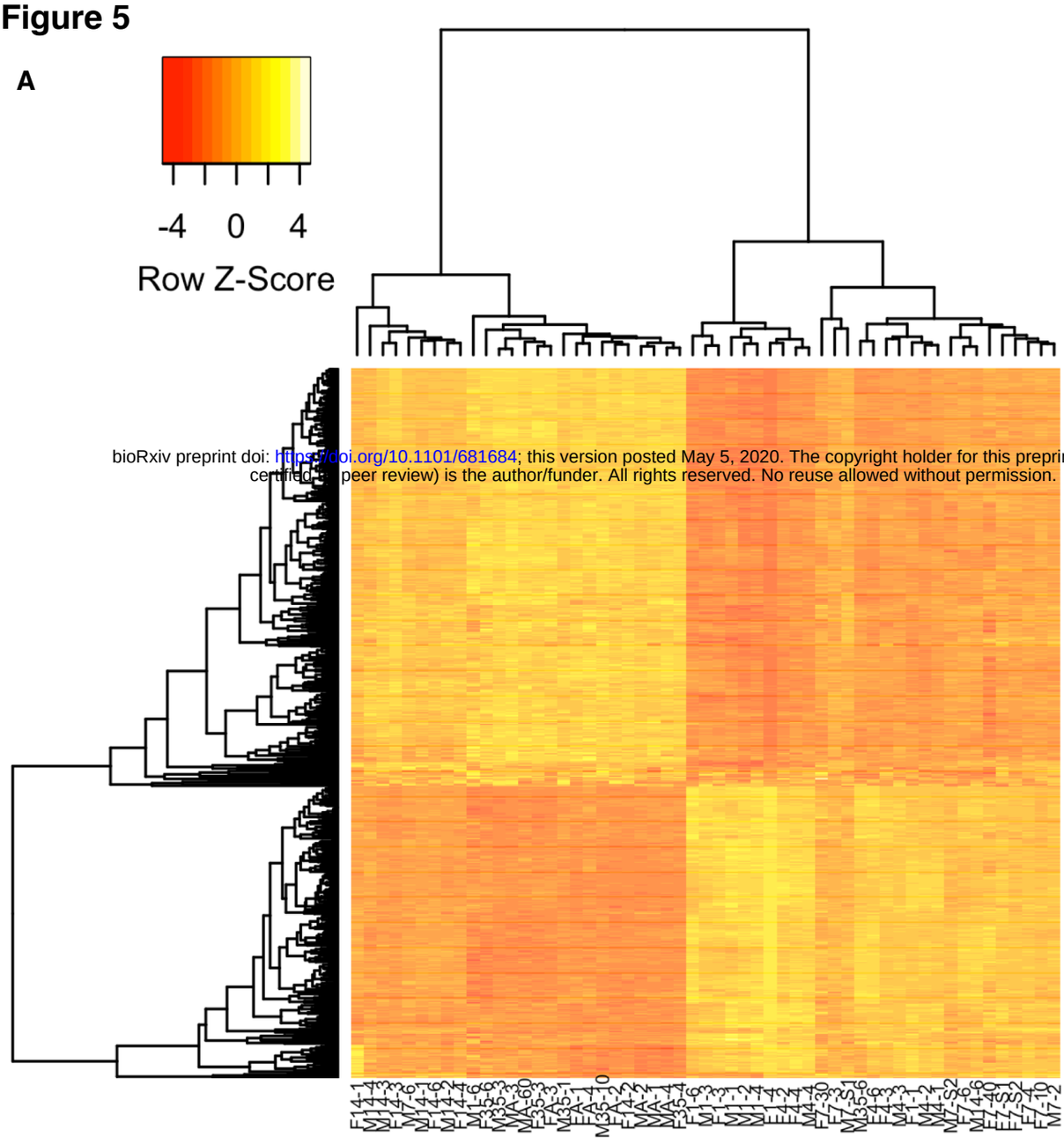

B

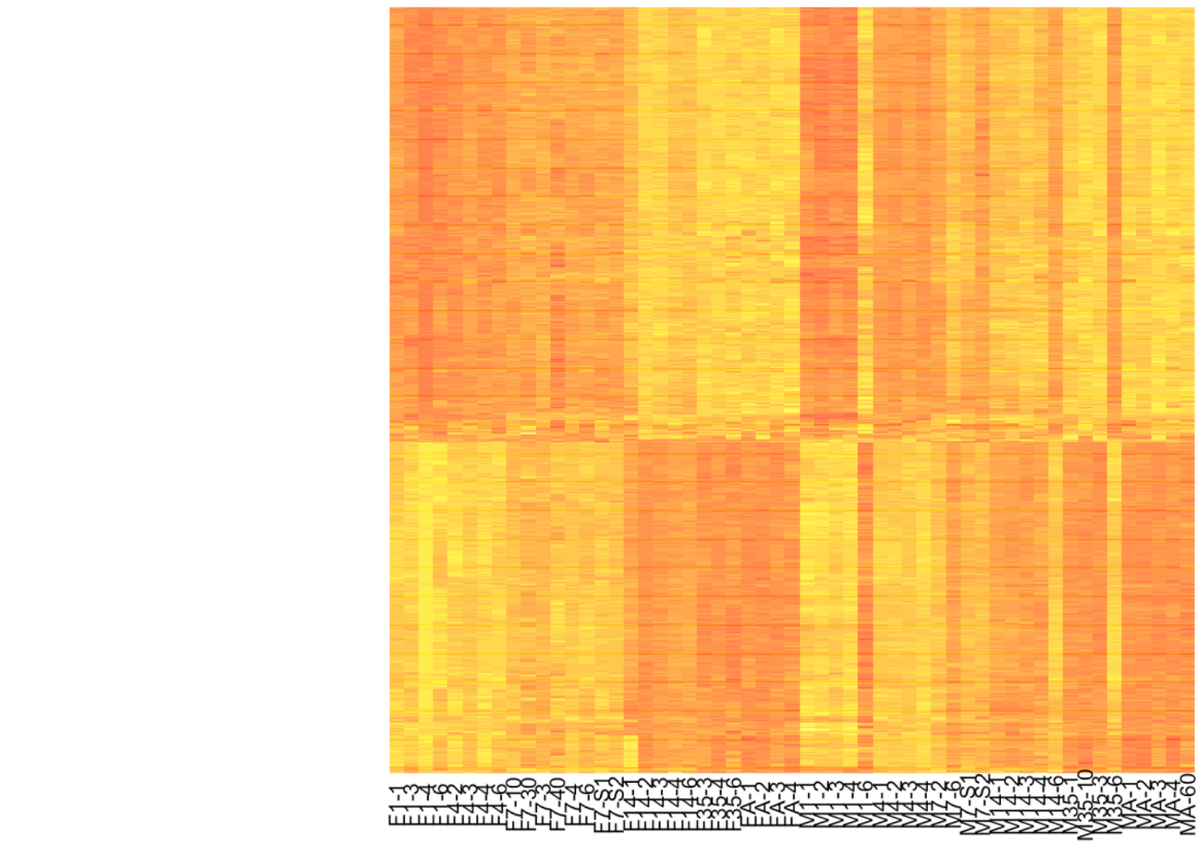

Figure 6

A

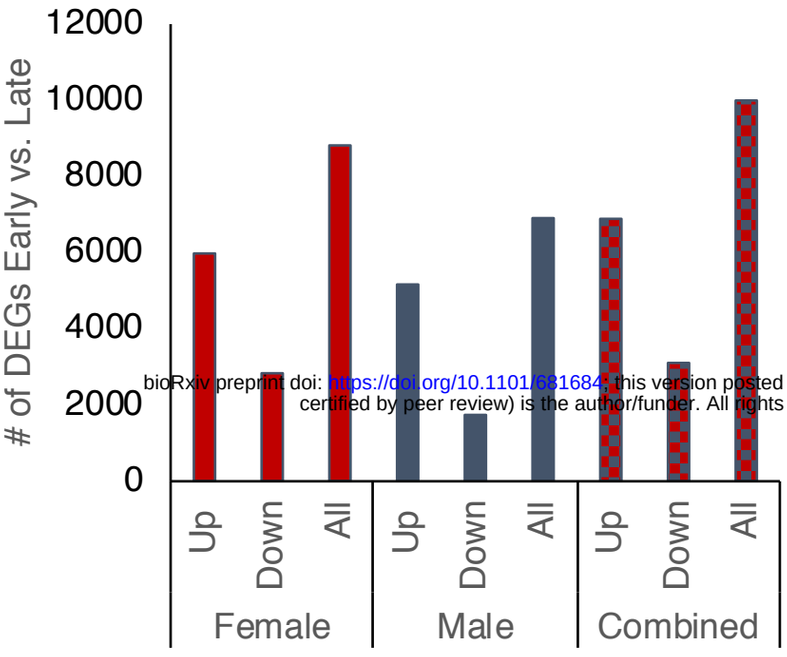

B

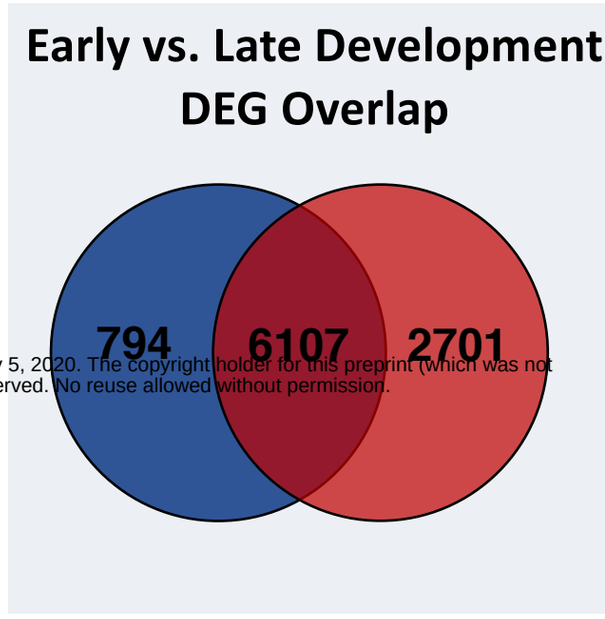

C

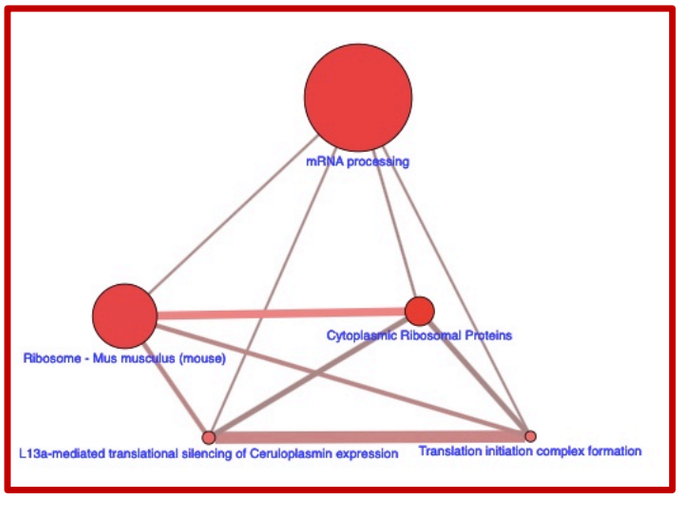

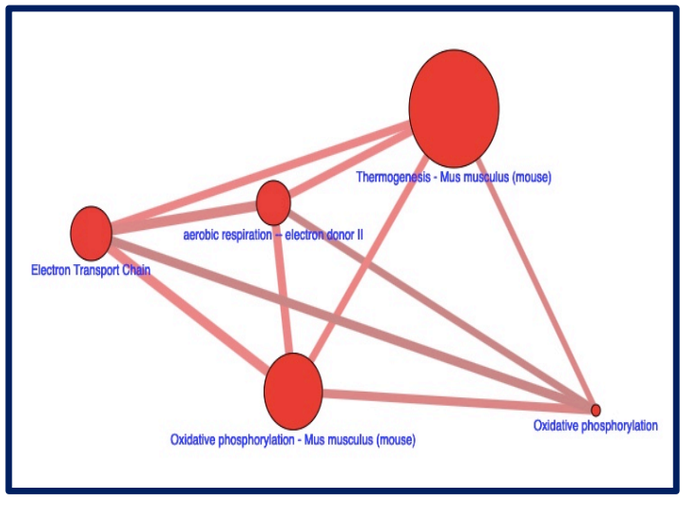

D

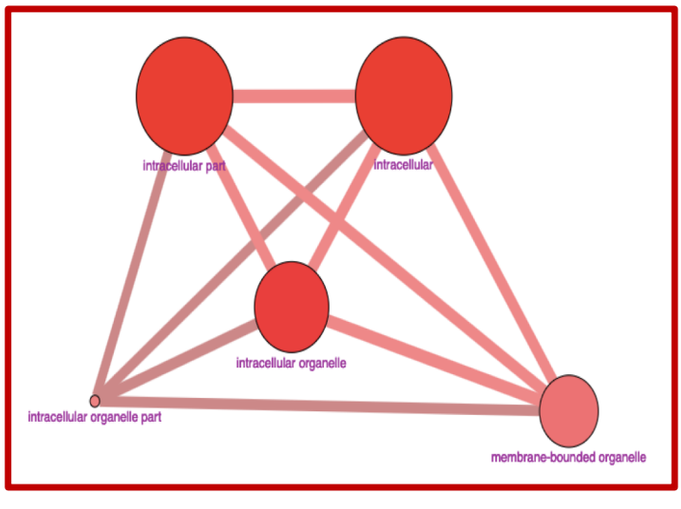

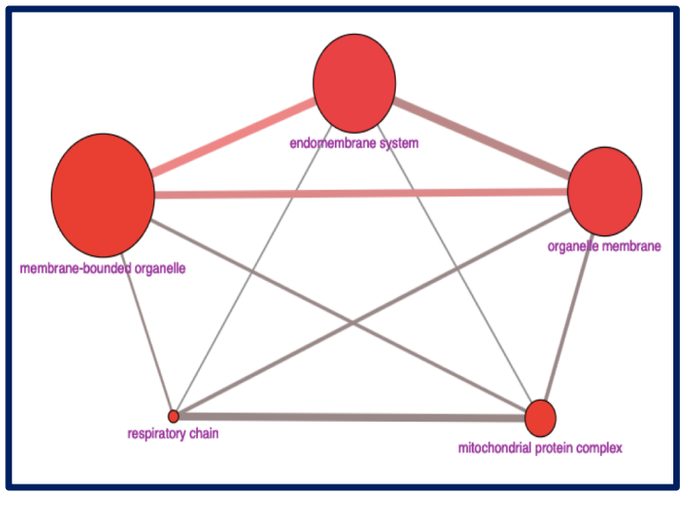

Figure 7

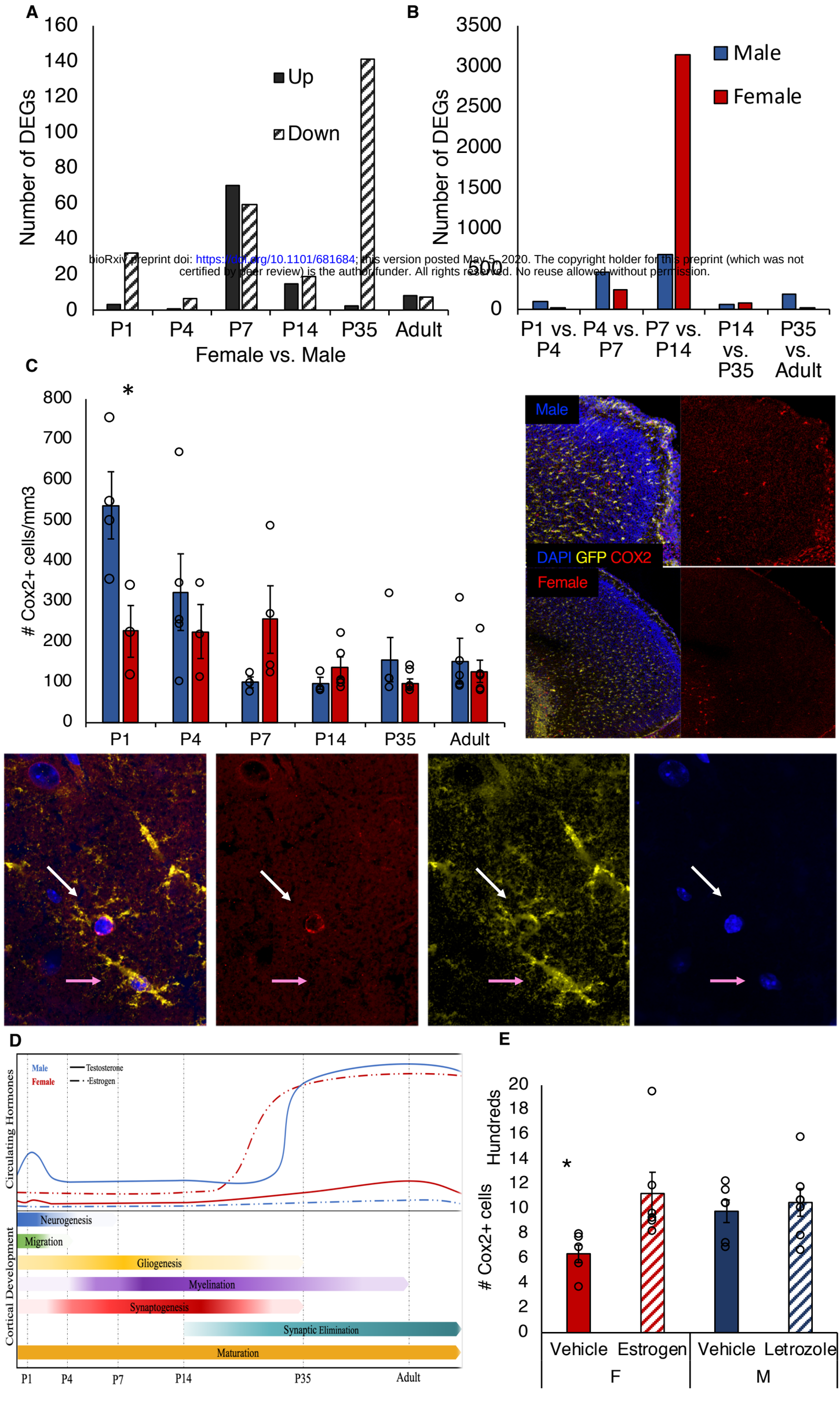

Figure 8

Astroglial- enriched modules

Male

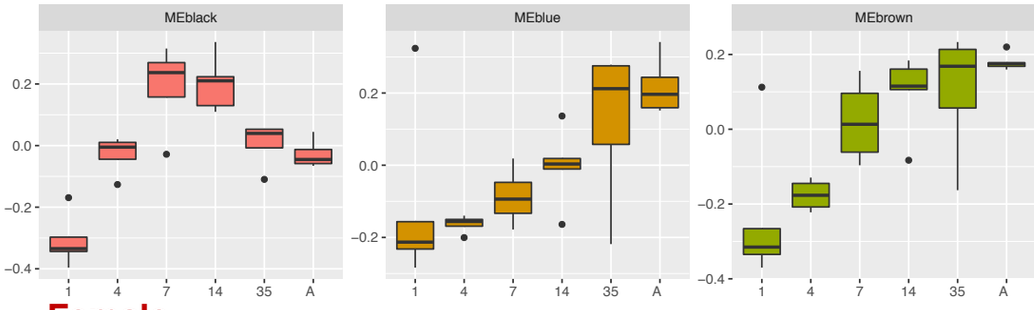

Female

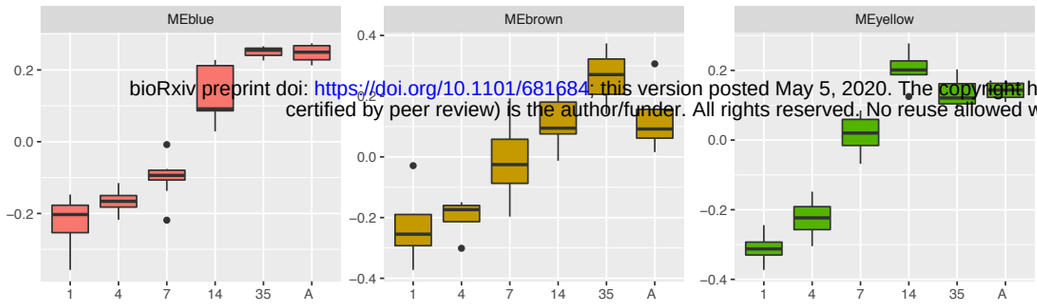

Cell Cycle- enriched modules

Male

Female

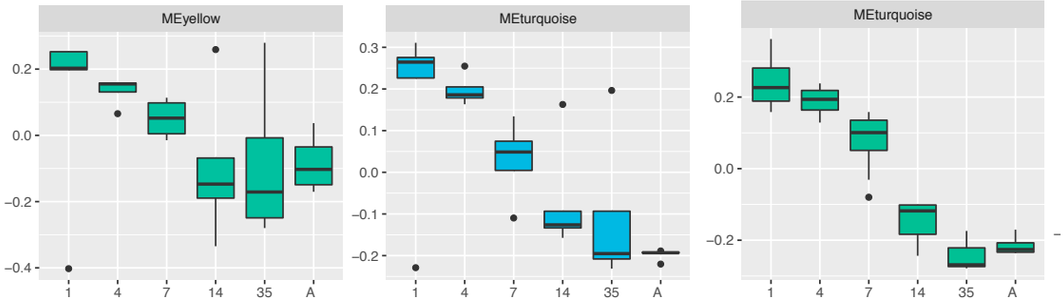

Mitochondria- enriched modules

Male

Female

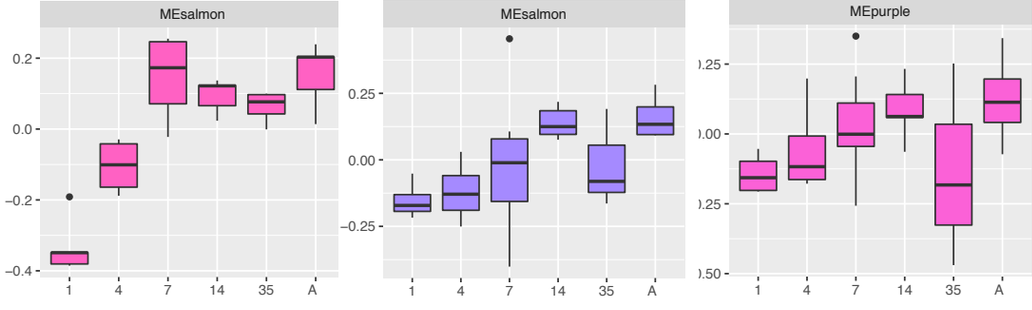

Translation- enriched modules

Male

Female